www.elsevier.com/locate/dsr2

Summer microbial community composition governed by upper-ocean stratification and nutrient availability in northern Marguerite Bay, Antarctica

Patrick D. Rozema, Tristan Biggs, Pim A.A. Sprong, Anita G.J. Buma, Hugh J. Venables, Claire Evans, Michael P. Meredith, Henk Bolhuis

PII: S0967-0645(16)30378-2
DOI: http://dx.doi.org/10.1016/j.dsr2.2016.11.016
Reference: DSRII4166

To appear in: *Deep-Sea Research Part II*

Cite this article as: Patrick D. Rozema, Tristan Biggs, Pim A.A. Sprong, Anita G.J. Buma, Hugh J. Venables, Claire Evans, Michael P. Meredith and Henk Bolhuis, Summer microbial community composition governed by upper-ocean stratification and nutrient availability in northern Marguerite Bay, Antarctica *Deep-Sea Research Part II,* http://dx.doi.org/10.1016/j.dsr2.2016.11.016

Summer microbial community composition governed by upper-ocean stratification and nutrient availability in northern Marguerite Bay, Antarctica

Patrick D. Rozema[a*], Tristan Biggs[b], Pim A.A. Sprong[a,1], Anita G.J. Buma[a,c], Hugh J. Venables [d], Claire Evans[b,e], Michael P. Meredith[d], Henk Bolhuis[b]

[a] Department of Ocean Ecosystems, Energy and Sustainability Research Institute, University of Groningen, Nijenborgh 7, 9747 AG, Groningen, The Netherlands

[b] Department of Marine Microbiology and Biogeochemistry, Royal Netherlands Institute of Sea Research, and Utrecht University, Landsdiep 4, 1797 SZ, 't Horntje (Texel), The Netherlands

[c] Arctic Centre, University of Groningen, Aweg 30, 9718 CW, Groningen, The Netherlands.

[d] British Antarctic Survey, High Cross, Madingley Road, Cambridge CB3 0ET, United Kingdom

[e] National Oceanography Centre, Waterfront Campus, European Way, Southampton, Hampshire SO14 3ZH, United Kingdom

Present address

[1] Alfred Wegener Institute for Polar and Marine Research, Am Handelshafen 12, 27570 Bremerhaven, Germany

* Corresponding author: P.D.Rozema@rug.nl

Keywords: Phytoplankton; Bacteria; Diatoms; macronutrients; MiSeq sequencing; glacial melt

Regional index terms: Antarctica; Antarctic Peninsula; Ryder Bay

Abstract

The Western Antarctic Peninsula warmed significantly during the second half of the twentieth century, with a concurrent retreat of the majority of its glaciers, and marked changes in the sea-ice field. These changes may affect summertime upper-ocean stratification, and thereby the seasonal dynamics of phytoplankton and bacteria. In the present study, we examined coastal Antarctic microbial community dynamics by pigment analysis and applying molecular tools, and analysed various environmental parameters to identify the most important environmental drivers. Sampling focussed on the austral summer of 2009-2010 at the Rothera oceanographic and biological Time Series (RaTS) site in northern Marguerite bay, Antarctica.

The Antarctic summer was characterized by a salinity decrease (measured at 15 m depth) coinciding with increased meteoric water fraction. Maximum Chl-a values of 35 µg l^{-1} were observed during midsummer and mainly comprised of diatoms. Microbial community fingerprinting revealed four distinct periods in phytoplankton succession during the summer while bacteria showed a delayed response to the phytoplankton community. Non-metric multidimensional scaling analyses showed that phytoplankton community dynamics were mainly directed by temperature, mixed layer depth and wind speed. Both high and low N/P ratios might have influenced phytoplankton biomass accumulation. The bacterioplankton community composition was mainly governed by Chl-a, suggesting a link to phytoplankton community changes. High-throughput 16S and 18S rRNA amplicon sequencing revealed stable eukaryotic and bacterial communities with regards to observed species, yet varying temporal relative contributions. Eukaryotic sequences were dominated by pennate diatoms in December followed by polar centric diatoms in January and February. Our results imply that the reduction of mixed layer depth during summer, caused by meltwater-related surface stratification, promotes a succession in diatoms rather than in nanophytoflagellates in northern Marguerite Bay, which may favour higher trophic levels.

1. Introduction

The Western Antarctic Peninsula (WAP) has recently experienced strong atmospheric warming. Between 1957 and 2006 the Antarctic Peninsula warmed by 0.11 ± 0.06 °C per decade and this increase was strongest during winter and spring (Steig et al., 2009; Turner et al., 2016). As a result, sea-ice extent has been decreasing in the WAP region, with potential consequences for phytoplankton bloom dynamics (Montes-Hugo et al., 2009). During spring and early summer, sea-ice melting may induce water column stratification enhancing the light availability for phytoplankton bloom development (Ackley and Sullivan, 1994; Sverdrup, 1953). Stratification in coastal regions is further promoted by increased freshwater supply from glacial melt and precipitation (Cook et al., 2016, 2005; Depoorter et al., 2013; Dierssen et al., 2002; Meredith et al., 2016, 2013, 2008; Rignot et al., 2013). Glaciers in the central and southern regions are affected most pronouncedly due to increasing temperatures of mid-depth (150 m) waters melting glacial fronts (Cook et al., 2016). Decreased cloud cover and increasing wind speeds in the northern WAP are further altering water column properties by changing light availability (Montes-Hugo et al., 2009). These changes are already affecting phytoplankton community dynamics and are likely to become more pronounced in the future (Moline et al., 2004; Montes-Hugo et al., 2009; Rozema et al., 2016; Saba et al., 2014).

Due to variability in regional warming, changes in the phytoplankton community and biomass are not uniform across the WAP (Montes-Hugo et al., 2009). Additionally, the ongoing retreat of glaciers along the WAP exposes new areas to light and consequently an increase in phytoplankton biomass (Peck et al., 2010). Wind speeds in the northern WAP are increasing, resulting in more pronounced mixing leading to lower surface chlorophyll a (Chl-a) levels (Montes-Hugo et al., 2009; Turner et al., 2005). In contrast, phytoplankton biomass is increasing towards the central/southern region of the WAP. In Marguerite Bay, an extensive bay surrounded by glaciers in the central region of the WAP, lower mean summertime sea surface temperatures and higher average Chl-a concentrations were observed when compared to the northern WAP (Clarke et al., 2008; Meredith et

al., 2010). The present study was conducted in Ryder Bay, in the northern part of Marguerite Bay, at the site of the Rothera oceanographic and biological Time-Series (RaTS).

The increase in glacial runoff affects the phytoplankton communities differently in various regions. In Potter Cove on King George Island (northern WAP), phytoplankton biomass remained low despite high nutrient levels (van de Poll et al., 2011). Here, sediment-rich run-off from the glacier increased water turbidity, thereby causing unfavourable irradiance conditions for phytoplankton growth despite salinity stratification. A similar scenario was described for Kongsfjorden on Spitsbergen (Arctic; Piquet et al., 2014). In contrast, glacial meltwater might contain high levels of iron thereby fuelling phytoplankton blooms (Bown et al., 2016; Gerringa et al., 2012). In the Amundsen Sea, high levels of phytoplankton biomass were sustained by iron input from the nearby Pine Island Glacier (Alderkamp et al., 2012).

The phytoplankton community in the central to southern WAP consists mainly of diatoms, the haptophyte Phaeocystis antarctica and cryptophytes (Annett et al., 2010; Buma et al., 2001; Garibotti et al., 2005; Kozlowski et al., 2011; Piquet et al., 2011). Diatoms are often dominant in stratified waters due to their adaptation to high irradiance levels while P. antarctica is mainly found in waters characterized by strong vertical mixing (Arrigo et al., 1999). Cryptophytes are thought to dominate waters strongly influenced by (glacial) meltwater (Moline et al., 2004). Earlier studies at the RaTS site reported peaks in phytoplankton biomass in December or January, possibly related to sea-ice presence and/or melt (Clarke et al., 2008; Venables et al., 2013). Additionally, a secondary Chl-a peak was frequently observed in March (Clarke et al., 2008). The phytoplankton summer community exhibited a succession of various diatoms (Annett et al., 2010; Buma et al., 2001; Clarke et al., 2008; Piquet et al., 2011). Also, both hetero- and autotrophic dinoflagellates accounted for 27% of the total phytoplankton biomass in Ryder Bay (Annett et al., 2010). Data on the abundance of haptophytes and cryptophytes in northern Marguerite Bay are limited but suggest that events which allow for the dominance of either of these two groups do not necessarily occur every summer (Annett et al., 2010; Arrigo et al., 1999; Moline et al., 2004; Piquet et al., 2011; Rozema et al., 2016). Previous

observations of the physical properties confirmed the representativeness of the RaTS monitoring site for the larger northern Marguerite Bay area (Venables and Meredith, 2014). This suggests that the previously described dynamics in the phytoplankton community should be applicable to the RaTS site.

The pivotal link between primary producers and higher trophic levels within the Antarctic food web is krill, which prefer grazing on (large) diatoms (Haberman et al., 2003; Quetin and Ross, 1985). Recent studies in the Southern Ocean have shown a decline in krill in favour of salps, presumably related to shifts in the phytoplankton community (Atkinson et al., 2004; Flores et al., 2012). This shift from krill to salps is not (yet) occurring at the WAP although these two grazers are not observed simultaneously (Steinberg et al., 2015). Other frequently observed grazers, yet considered of less importance or less well studied, are copepods, (silico)flagellates, heterotrophic dinoflagellates and tintinnids (Atkinson et al., 2012; Dolan et al., 2013; Ducklow et al., 2012a; Sherr and Sherr, 2007; Steinberg et al., 2015). Potentially, grazers could exert top-down control on the phytoplankton biomass in the WAP ecosystem (Behrenfeld, 2010). A recent investigation into the applicability of this mechanism, the so-called 'dilution-recoupling hypothesis', for the RaTS site suggests that phytoplankton biomass accumulation is more strongly linked to light than grazing pressure (Venables et al., 2013). Yet incidentally strong governance of phytoplankton biomass by grazers during summer periods cannot be excluded.

Bacterial community dynamics seem to be mostly dependent on phytoplankton biomass and composition (Delmont et al., 2014; Kim et al., 2014; Landa et al., 2016). Antarctic marine bacterial biomass correlates with recently produced algal dissolved organic carbon (DOC; Moran et al., 2001) while marine bacterial community composition correlated with the concentration and speciation of dissolved organic matter (DOM; Billen and Becquevort, 1991; Ducklow et al., 2012b; Landa et al., 2016). Furthermore, a shift in bacterial community composition was shown to follow a shift in phytoplankton composition, with a lag phase lasting a few days to one month (Billen and Becquevort, 1991; Ghiglione and Murray, 2012; Piquet et al., 2011). The bacterial community in marine Antarctic

habitats consists mainly of the phyla (Alpha- and Gamma-) Proteobacteria, Actinobacteria and Bacteroidetes (Delmont et al., 2014; Gentile et al., 2006; Kim et al., 2014; Landa et al., 2016; Luria et al., 2014; Piquet et al., 2011). The Bacteroidetes are also referred to as the Cytophaga-Flavobacterium-Bacteroides (CFB) group (Abell and Bowman, 2005; Gentile et al., 2006). One study based on metaproteomics revealed a dominance of Rhodobacterales and Alteromonadales (Williams et al., 2012). The Sulfitobacter genus (Rhodobacterales) was observed to increase in relation to DOM of diatom origin (Landa et al., 2016). This genus, and other genera belonging to Rhodobacterales, are known to be able to transform DMSP, observed in high quantities at RaTS (Stefels, personal communication), into DMS (Curson et al., 2008; Reisch et al., 2011). Furthermore, during winter bacterioplankton diversity was found to be higher compared to summer (Ghiglione and Murray, 2012; Ladau et al., 2013).

The aim of this study was to understand how the microbial community in Ryder Bay (Adelaide Island, WAP) responds to changes in environmental conditions. We hypothesized that both phytoplankton and bacteria are governed by enhanced water column stability caused by sea-ice melt during spring and/or glacial meltwater input during summer (Clarke et al., 2008; Meredith et al., 2010). Furthermore, we hypothesized that limitation by macronutrients would be unlikely (Bown et al., 2016; Clarke et al., 2008; Venables et al., 2013). Finally, we hypothesized that the bacterial community changes, albeit with a delay, due to shifts in phytoplankton community composition.

To test our hypotheses, we followed microbial community structure at the RaTS site in northern Marguerite Bay during the summer of 2010-2011. We applied an approach which combined two DNA (Denaturing Gradient Gel Electrophoresis (DGGE) and MiSeq amplicon sequencing) and two pigment-based techniques (High pressure liquid chromatography (HPLC) and size-fractionated Chl-a).

2. Material and methods

2.1 Study site and sample collection

This study was conducted in Ryder Bay, Adelaide Island (Western Antarctic Peninsula) near Rothera research station (Fig. 1). Sampling took place at the RaTS site (67°34.200'S 68°13.500'W, fig. 1), ~4 km from Rothera (Clarke et al., 2008). Sampling (excluding collection of DNA samples, see below) occurred once or twice a week in the period from October 15, 2010 to March 23, 2011 from a small boat equipped with a hand winch. Full water column profiles were obtained with a CTD (conductivity, temperature, and depth) supplemented with LiCor photosynthetically available radiation (PAR) and fluorescence sensors (WetLabs). Calibration of the CTDs between years and with the Palmer Long-Term Ecological Research (LTER) program (Ducklow et al., 2012a) are discussed in Venables et al. (2013). Samples for HPLC analysis of pigments, nutrients (nitrate, nitrite, phosphate and silicate), size-fractionated Chl-a (>20 µm, 20-5 µm, 5-2 µm and 2-0.2 µm) and $\delta^{18}O$ were taken at water depth (15 m) using a 12 L Niskin bottle as part of the standard RaTS sampling scheme. This depth represents the long-term climatological phytoplankton peak observed using a fluorescence sensor attached to the CTD (Clarke et al., 2008). Sample processing for nutrients, $\delta^{18}O$, and size-fractionation was done according to the RaTS standard protocol (Clarke et al., 2008; Meredith et al., 2008). For HPLC, 1000 mL was filtered over 47 mm GF/F filters (Whatman, US). Filters were snap frozen in liquid nitrogen and stored at -80 °C for later analysis in the home laboratory.

For DNA analysis, seawater samples were taken at 15 m depth on December 9, 2010 and January 13, 24, 27, 31, February 3, 10, 16, and 21 (2011). Between 2 and 4 litres, collected as described above, were filtered on a 47-mm polycarbonate membrane of 0.2 µm pore size (Millipore, US). Filters were snap frozen in liquid nitrogen and stored at -80 °C until analysis in The Netherlands.

2.2 Analytical procedures

2.2.1 Environmental parameters (RaTS-programme)

Mixed-layer depth (MLD) was calculated as the depth where the density difference (Δσ) relative to the surface was 0.05 kg m^{-3} (Brainerd and Gregg, 1995). Salinity is presented on the practical salinity scale. Five-day averaged wind speed data from Rothera station was retrieved from the British Antarctic Survey (http://www.antarctica.ac.uk/met/metlog/). Nutrient samples were analysed in the UK according to Clarke et al. (2008). Oxygen isotope samples ($\delta^{18}O$) were analysed as described in Meredith et al. (2008) at the Natural Environment Research Council Isotope Geosciences Laboratory (Keyworth, UK).

2.2.2 Pigment analysis (RaTS-programme)

Size-fractionated Chl-a samples were classified and analysed on base as described before (Clarke et al., 2008) following Wood (1985); in short, pigment extractions were performed overnight at 4° C in chloroform/methanol (2:1 v/v) and Chl-a was determined before and after the addition of 0.1 N HCl using a fluorometer (AU-10, Turner). The microplankton (>20 µm) fraction was calculated from the size-fractionated Chl-a data and normalized to HPLC Chl-a values. Samples for HPLC analysis, as part of the RaTS program (Rozema et al., 2016), were processed as described in van Heukelem and Thomas(2001) and modified by Perl (2009). In short, HPLC filters were freeze dried for 48 hours. Pigments were extracted in 90% acetone for 48 hours in the dark and at 4 °C. Pigment detection was run on an HPLC (Waters 2695 separation module, 996 photodiode array detector) equipped with a Zorbax Eclipse XDB-C_8 3.5 µm column (Agilent Technologies). Quantification was done using standards (DHI, Denmark). Pigments reported in this study are: Chl-a, chlorophyll b, chlorophyll c_3, peridinin, 19'-butanoyloxyfucoxanthin, fucoxanthin, neoxanthin, prasinoxanthin, 19'-hexanoyloxyfucoxanthin, alloxanthin and lutein. Initial and final pigment ratios are presented in Table A.1. Values for Chl-a reported in this study were based on HPLC analysis.

2.2.3 DNA extractions

DNA was extracted from the filters using a modified protocol of Boelen et al. (2000). Microcentrifuge tubes (1.5 mL) containing halved filters were filled with 500 µL DNA extraction buffer (2% [w/v] cetyl trimethylammonium bromide (CTAB), 1.4 M NaCl, 20 mM EDTA, 100 mM Tris-HCl (pH = 8.0) and heated to 60 °C. One µL (beta)-mercaptoethanol was added before incubation for 30 minutes at 60 °C. Samples were centrifuged for 10 minutes at 14k rcf, after the addition of 500 µL CIA (Chloroform/Isoamylalcohol [24:1] v/v). The upper phase was transferred to a clean tube. Subsequently, 335 µL isopropanol was added and the samples were cooled for one hour at 4 °C. The samples were centrifuged for 30 minutes at 14k rcf and 4 °C, after which the liquid phase was discarded. The pellet was cleaned in 800 µL ethanol (80%) before incubation at -20 °C for 10 minutes. The ethanol was discarded after centrifuging for 30 minutes at 14k rcf and 4 °C. Pellets were dried for ~60 minutes at room temperature before resuspension in 100 µL of 0.1x TE buffer (1 mM Tris-HCl, 0.1 mM EDTA, pH 8.0). Finally, the DNA samples were incubated overnight at 4 °C to dissolve and stored at -20 °C.

2.2.4 DNA amplification

PCR reactions (25 µL final volume) were run on a VWR thermo cycler (VWR, US). For every reaction, 2.5 µL of a 10- to 100-fold diluted DNA solution was used as a template. The following primer sets were used: Euk1A and 516R-gc for eukaryotes (Amann et al., 1990; Díez et al., 2001; Sogin and Gunderson, 1987), diatom specific primer Diatom18SR1 and 1209F-GC (Giovannoni et al., 1988; Godhe et al., 2008), Dino 18S F1-GC and Dino 18S R1 for dinoflagellates (Lin et al., 2006) and 968F-GC and 1401R for bacteria (Nübel et al., 1996). The –GC suffix stands for the GC-clamp required for analysis by DGGE. Additional information on the primers used can be found in Table A.2 and reaction mixture composition and reaction conditions are listed in Table A.3. Amplicon yield was estimated by DNA gel electrophoresis on a 1% agarose gel, stained with ethidium bromide (0.002 %). Gels were visualized using an Image Master (Pharma Biotech, UK). DNA amplicon yield and size were estimated by including a DNA Smart Ladder (Eurogentec, Belgium).

2.2.5 DGGE

PCR product was subjected to DGGE analysis using a PhorU system (Ingeny, Netherlands). DGGE analysis was done as described in Piquet et al. (2008). Approximately 60 ng of PCR amplicon was run for each sample as well as in-house developed markers with bands along the gradients of interest. Different denaturing gradients of urea-formamide were used; 20-45% for diatoms and eukaryotes, 20-40% for dinoflagellates and 30-70% for bacteria. All samples were run for 16 hours at 100V in 0.5x TAE buffers, except for the diatom samples, which were run for 20 hours. The gels were stained using silver staining, according to Heuer et al. (2001).

2.2.6 Community sequencing

Analyses of the species composition in both the eukaryotic and bacterial fractions using MiSeq were performed on samples representative of the various periods in microbial succession as judged from DGGE clustering (general Eukaryotes and Bacteria; Fig. 6 & 7). This resulted in three representative DNA samples (December 9, January 27 and February 16) that were shipped on dry-ice to the Research and Testing Laboratory (Texas, United States) for paired-end sequencing on an Illumina MiSeq using their protocols and primers. The EukA7F and Euk555R primers were used to investigate the eukaryotic community while 28F and 519R were used for the bacterial community (Table A.2; Frank et al., 2013; Medlin et al., 1988; Moreno et al., 2010).

2.3 Data analysis

2.3.1 RaTS parameters

CTD data were visualized in Ocean Data View v4.5.6 (Schlitzer, 2013). Correlations between environmental parameters were calculated in the statistical package PAST v2.17c (Hammer et al., 2001). The CHEMTAX analysis package v1.95 (Mackey et al., 1996) was used to calculate relative and

absolute abundances of different phytoplankton groups based on the pigment concentrations as obtained by HPLC. Phytoplankton group abundances were calculated in CHEMTAX by groups using marker pigments and their previously derived ratios. The program then uses a factor analysis and steepest descent algorithm to find the best fit based on initial pigment ratios. The phytoplankton groups used in our analysis were: prasinophytes, chlorophytes, dinoflagellates, cryptophytes, two classes of haptophytes (P. antarctica has a variable pigment signature in response to iron conditions (van Leeuwe et al., 2014)), and two classes of diatoms. Diatoms were separated as one class with Pseudonitzschia-like species containing chlorophyll c_3 while the other class does not. Initial ratios (Table A.1) were obtained from Wright et al. (2010), except those for P. antarctica, which were taken from Wright et al. (2009). After CHEMTAX analysis, abundances for both haptophyte and both diatom classes were pooled and presented as haptophytes and diatoms, respectively.

2.3.2 Calculation of freshwater origin

The ratio of oxygen isotopes ($\delta^{18}O$) in the sea water samples was used to subdivide the freshwater fraction, as calculated from salinity measurements, into quantitative estimates of freshwater contributions from sea-ice melt and meteoric water. This distinction is possible as freshwater of meteorological origin is isotopically lighter than freshwater originating from sea-ice melt. The two sources of meteoric water are precipitation and glacial melt water input (Craig and Gordon, 1965). The relative balance of direct precipitation and glacial discharge is discussed in detail in Meredith et al. (2016); for the period of our data, the latter is inferred to be the dominant freshwater input.

2.3.3 Analysis of community fingerprints from DGGE

The DGGE gels were digitized using a negative photo scanner (Epson Perfection V700 photo). Bionumerics v3.5 (Applied Maths, Belgium) was used for analysis of the DGGE band patterns as described in Piquet et al. (2008). We used the in-house developed markers to ensure correct

alignment of bands between samples. Band patterns were transformed to relative band intensities and exported to Past v2.17c (Hammer et al., 2001) to estimate species evenness and richness, and Simpson diversity indices (Simpson, 1949). The Simpson indices were subtracted from 1.

Furthermore, the DGGE data were analysed using the Bray-Curtis similarity coefficient and presented in the form of unweighted pair group method with arithmetic averages (UPGMA) dendrograms. One of the markers used for the DGGE was added as outgroup. Values for the cophenetic correlation were deemed good if >0.85. Each dendrogram underwent bootstrapping (n = 1000). Bootstrap values, the percentage of replicates in which each node was present, were added to the dendrograms. These bootstrap values were consequently used to propose clusters with a certain degree of confidence. NMDS (Non-metric multidimensional scaling) was chosen to explore how the community data based on DGGE related to each other at the different time points during the Antarctic summer season (reviewed in Ramette (2007)). The relative band intensity was also used for NMDS. The minimum spanning tree was added to show the nearest neighbour of every sample within multidimensional space as we simplified the NMDS to a 2d plot. Stress of the ordination was checked using Shepard plots. Finally, we added vectors to the NMDS for a number of (environmental) parameters to create a biplot to identify which variables potentially influenced the microbial communities. These variables were not included in the ordination and are simply a projection of the variable along a linear vector. The length of the vectors was scaled linearly to improve the visual interpretation of the NMDS biplot, so only their directions and relative lengths should be considered (Ramette, 2007). We used the following environmental variables for the eukaryotes, diatoms and dinoflagellates NMDS's; PAR, MLD, wind speed, salinity, water temperature, total N (nitrite and nitrate summed), phosphate and silicate. Silicate was excluded for the dinoflagellates. For bacteria, Chl-a was added as a proxy for algal biomass.

2.3.4 Community sequence analysis

Amplified 16S and 18S rRNA gene sequence reads were analysed using a number of algorithms within the QIIME microbial community analysis pipeline (Caporaso et al., 2010). Paired reads were pre-processed and joined using PEAR (Zhang et al., 2014). A quality filter step was used to filter out reads with ambiguous bases, unrealistic read lengths and reads with an average quality scores (using a 40 nt sliding window) below 30. Mapping, dereplication, OTU clustering and chimera checking/removal were done using Vsearch 1.1.3 (Torbjørn et al., 2015). For OTU clustering we choose a 95% sequence identity cut off to accommodate for the higher expected variation in the variable regions which would lead to an overestimation of the actual diversity when the traditional 97% cut off would be used. The cluster centroid for each OTU was chosen as the OTU representative sequence and OTU's with an occurrence smaller than 6 in the complete dataset were removed before community analysis. The taxonomic assignment of the representative sequences was carried out using a naïve Bayesian classifier (Wang et al., 2007) against the SILVA SSU non-redundant database (119 release; Quast et al., 2013). Diatoms in this database are ordered as proposed recently (Medlin and Kaczmarska, 2004). BIOM tables generated by the taxonomic assignment yielded seven taxonomic levels for bacteria and eight for eukaryotes ranging from phyla to family or genus ranks. Nodes representing >1% of the data set with the three samples combined are presented in this manuscript while the full list is included in Table A.4. DNA sequences obtained in this study are deposited in the National Centre for Biotechnology Information (NCBI) Sequence Read Archive under accession number SRP072539.

3 Results

3.1 Environmental variables

Spring (October-November) was characterized by a deep mixed layer (~80 m; Fig. 3) and major nutrients were abundant with phosphate and total nitrogen concentrations around 1.3 and 16 µM

respectively (Fig. 4). The deep MLD suggesting that the source of nutrients replenished during winter was deep mixing maintained by strong and persistent winds (Fig. 3). At the start of summer (December), the water column quickly stratified due to a strong decrease in salinity, ranging between 33.1 and 33.8 (Fig. 2). Lowest salinities observed were 33.3 on January 27 and 33.1 on February 21. Density changes were strongly related to changes in salinity ($r^2 = 0.98$, $p < 0.001$) and not temperature, as is inevitable given the equation of state for seawater at low temperature. During the period of DNA sampling, the water column slowly warmed from -0.7 °C on December 9 to >1.5 °C at 15 m in the period from January 26 to February 4. PAR decreased during the DNA sampling period (data not shown). Throughout the summer, maximum PAR at 15 m was 111.5 µmol photons m^{-2} s^{-1}. PAR values during the sampling period for DNA analyses were 46.9 µmol photons m^{-2} s^{-1} on December 9 and a maximum of 12.3 µmol photons m^{-2} s^{-1} in January and February. CTD fluorescence signals revealed two peaks during DNA sampling (Fig. 2). Fluorescence values at 15 m reached peak values on December 28 (22 mg Chl-a m^{-3}) and January 17 (27 mg Chl-a m^{-3}). A second fluorescence peak was observed on February 7 (9.3 mg Chl-a m^{-3}). During DNA sampling the MLD was shallow (<10 m; Fig. 3). Fluorescence peaks were therefore found below the MLD except for a short period from December 31 to January 8. During this period the MLD deepened to a maximum of 31 m on January 4, coinciding with an increase in wind speed, starting December 11 and decreasing after January 4. A maximum wind speed of 8.0 m s^{-1} was observed on December 28. The decrease in salinity over the season correlated strongly with an increase in meteoric water (glacial melt plus precipitation), based on $\delta^{18}O$ results ($r^2 = 0.74$, $p < 0.001$, Fig. 3). In contrast, no sea ice was present in Ryder Bay during the period of interest (Venables et al., 2013). Only brash ice of glacial origin was observed frequently in December and occasionally in January and February (data not shown). In theory, the increase in meteoric water could represent increased glacial discharge or increased input of precipitation, with the latter including the injection to the ocean of snow that had accumulated on top of sea ice during winter. However, the absence of sea ice from Ryder Bay during the study period precludes this and glacial discharge and the melt of snow accumulated on land is inferred to be the likely dominant

source of meteoric water input (Meredith et al., 2016). Total N and phosphate reached minimum values on January 27 (1.1 µM) and February 3 (0.1 µM) respectively (Fig. 4). Silicate showed no clear seasonal pattern. However, two minima were observed: on January 10, (22.2 µM) and on March 7, (23.4 µM). At the end of the season, values returned to those found at the beginning of the season. The average N/P ratio over the summer was 13.0 and was relatively stable apart from two deviations. Firstly, the ratio increased from December 17 to 28 to a maximum of 26.4 before restabilising at the average on the 31st. Secondly, N/P ratios decreased below 10 on January 17 and fell to 5.3 on January 27. Thereafter, the ratio increased back to its average.

3.2 Phytoplankton pigments

HPLC based total Chl-a concentration revealed two biomass peaks during the DNA sampling period (Fig. 5) as suggested earlier by the two in situ fluorescence maxima (Fig. 2). The main component of total Chl-a consisted of the microplankton fraction: over the entire HPLC sampling period, total Chl-a consisted on average of 78.6% microplankton (Fig. 5). The remaining 21.4% was evenly divided across the three smaller fractions. Phytoplankton community diversity was higher at the start of the HPLC sampling period and decreased over the sampling period.

The phytoplankton community was diverse during spring (October-November; Fig. 5). Initially, haptophytes were more dominant (46%) than diatoms but these were steadily replaced by diatoms over the course of spring resulting in a relative abundance of <10%. Also, prasinophytes were a major component of the community, contributing on average 16% during spring. Cryptophyte relative abundances were low averaging only 6%.

During summer, dinoflagellates and prasinophytes were not major contributors to the phytoplankton community. Only after January 17 was there a slight increase in absolute and relative abundance of these two groups. Chlorophyte contributions were low throughout the season. During the first Chl-a peak, diatoms became the dominant phytoplankton group. This group remained

dominant until the end of the summer. Relative contributions of cryptophytes and haptophytes remained low during summer although three modest temporary increases in absolute cryptophyte abundance occurred. These increases coincided with observed dynamics in Chl-a although the contribution of cryptophytes peaked at 1.02 µg Chl-a l^{-1}. Absolute haptophyte abundance only increased once (to 0.28 µg Chl-a l^{-1}) during the period of the highest Chl-a concentration (January 20).

3.3 Molecular fingerprinting

3.3.1 Eukaryotes

DGGE analysis revealed 21 to 34 bands in each sample (Table 1). Evenness ranged from 0.64 to 0.83, and was lowest at the start of summer or when Chl-a was >8 µg l^{-1}. Values for the Simpson index varied little, from 0.92 to 0.95. The dendrogram showed strong separation of the December 9 and February 21 samples: both samples deviated highly from the other samples (Fig. 6). Furthermore, one cluster consisted of January 13, 24, 27, 31 and February 3 samples (Euk1). A second cluster consisted of the February 10 and 16 (Euk2) samples. Similarity between clusters Euk1 and 2 was 0.60. Within Euk1 there was a weak indication of two distinct clusters (January 13 and 25 vs January 27, 31 and February 3) but only 39% of the replicates supported this separation. NMDS results did support the observations made with the UPGMA and the minimum spanning tree suggested a pattern of seasonal succession (Fig. 6). The biplot supported the trends in environmental parameters as water temperature increased during January 24 and February 3. The weak separation within the Euk1 UPGMA cluster was apparent in the NMDS. The wind mixing event during the first half of February, followed by a deepening of the MLD, seemed to be the main driver for the separation of clusters Euk1 and 2. The beginning (December 9) and end of the season (February 21) were opposed in both biological and environmental parameters judging from their opposite positions in the NMDS.

3.3.2 Diatoms

Each sample contained 8 to 16 diatom-related DGGE bands (Table 1). There was no obvious trend in the Simpson indices but overall values were low (mean = 0.84) and variable (standard deviation = 0.04). The evenness was low, ranging from 0.56 to 0.78, and showed an increasing trend over the duration of the season. The only noteworthy deviation in the average number of diatom species was January 31 (8; mean 12.8). The diatoms showed weak clustering by date (Fig. 6): only January 24 showed a unique composition. As opposed to the eukaryotes, December 9 and February 21 (Dia1) were moderately similar to each other and dissimilar to the other time points. NMDS supported the weak clustering as observed in the UPGMA as distances between samples appeared to be relatively equal. Of the four NMDSs performed, R^2 (0.71) of the diatoms was lowest. The vectors of the environmental parameters showed no clear trends with the eukaryote fingerprinting results other than salinity and phosphate having the longest vectors.

3.3.3 Dinoflagellates

Analysis of the DGGE banding pattern showed a stable community from 17 to 24 species per sample (Table 1). Variability in the Simpson indices was low and thus relatively stable. In contrast, evenness varied more, from 0.55 to 0.78, and slowly increased towards the end of summer. The strongest increase was at the end of January, during the decay of the largest peak in Chl-a and coinciding with an increase in absolute abundance of dinoflagellates as derived from pigment analysis. The dendrogram revealed three unique communities: December 9, January 13 and February 21 (Fig. 7). Community composition was relatively stable during the period from January 24 to February 16, with all communities showing >65% similarity. Most samples were oriented along the vertical axis in the NMDS, where salinity and MLD were found to be most strongly correlated (Fig. 7).

3.3.4 Bacteria

The number of bands observed in the DGGE gel ranged from 21 to 29 per sample (Table 1) with the highest number on January 27, slightly decreasing over the course of the summer. Overall, Simpson indices first increased during December and January reaching a peak value on January 31, thereafter diversity decreased slightly (min-max = 0.86-0.93). Interestingly, the lowest diversity was also observed in the second half of January, namely January 24. Evenness ranged from 0.58 to 0.80. The highest value was measured on January 31 and coincided with low phytoplankton biomass. The dendrogram showed clustering of the samples of December 9 and January 13 (Bac1; Fig. 7). Similarity between the two samples was 0.69. A second cluster consisted of January 24 and 27 samples (Bac2) while a third cluster included samples taken on January 31 and February 3, 10 and 16 (Bac3). February 21 clustered with Bac3 for 48% of the permutations. The similarity between clusters Bac2 and 3 was 0.60. NMDS showed a strong correlation between Chl-a and bacterial community composition. Furthermore, the remaining vectors suggested a similar distribution as observed in the eukaryote NMDS. The minimum spanning tree showed relative large distances between the sampling dates, fully supporting the clustering proposed in the UPGMA. The biplot showed clustering of January 24 and 27, mainly driven by phytoplankton biomass (Fig. 7). December 9 and January 13 clustered based on high PAR and elevated nutrient concentrations.

3.4 Community sequences

3.4.1 Eukaryotic sequences

The total number of observed nodes to which sequences could be assigned with a ≥95% similarity was 45, 49 and 50 in December, January and February respectively. Species evenness was generally low, but highest in December (0.26) with respect to the two later samples (0.20 and 0.15). Simpson indices followed the same trend as evenness and dropped from 0.84 to 0.75. Results of the eukaryotic sequences support the clustering as shown by DGGE analysis. January 27 and February 16 samples were more similar in community composition (73%) in comparison to December 9 (42%,

UPGMA, data not shown). December 9 was dominated by unknown pennate diatoms (Bacillariophyceae), which were hardly observed in the two later samples (Table 2). In contrast, polar centrics (Mediophyceae), represented by the genera Thalassiosira and Chaetoceros, increased in abundance in the three consecutive samples (Fig. 8). Radial centrics (Coscinodiscophyceae) were hardly observed and only represented by Stellarima microtrias. Haptophytes were the only representatives of the Prymnesiophyceae. Their abundances were lowest on December 9 (0.6%) and doubled in the following two samples (1.21-1.24%). Also, cryptophytes were only represented by the order of Cryptomonadales and slightly decreased from 1.59 to 0.08% during the summer. Dinoflagellates were observed in high numbers throughout the season. The maximum percentage of sequences allocated for dinoflagellates (or Alveolata, Dinophyceae, Gymnodiniphycidae) was on January 27 with 34.49% while only 20.04 and 21.06% of the sequences were related to dinoflagellates on respectively December 9 and February 16. Both MAST-4 and MAST-1 stramenopiles were observed. The first group had 3.21% of the sequences on December 9 and decreased to <0.25% for the later samples. Mast-1 remained constant at ~0.4% of the sequences.

Apart from heterotrophic dinoflagellates, the non-photosynthesizing community was represented most significantly by species from the order Maxillopoda to which the suborder Copepoda belongs (Table 2). While almost absent in December (0.05%) and January (0.50%), it was well represented in February where 8.44% of the sequences were allocated to this order. Further potential grazers were ciliates belonging to Oligotrichia and Choreotrichia (possibly including tintinnids), and both groups were most abundant (max 2.01%) on December 9. Finally, two nodes with single-celled amoeboid protists were observed, including Protaspa, belonging to the class of Thecofilosea. The relative abundance of amoebas was highest on December 9 and decreased during the season. A dinoflagellate endosymbiont (Syndiniales group 1) completed the list of nodes with >1% of the sequences but the only noteworthy contribution was on December 9 (1.32%).

3.4.2 Bacterial sequences

The majority (60-75%) of the sequence reads obtained using the Bacteria specific primers could be assigned as chloroplasts and were ignored in further analysis of bacterial diversity. The most abundant groups of the remaining sequences were assigned as Proteobacteria and Bacteroidetes (data not shown). A significant part of the sequences (2-11%) could not be assigned at the phylum level. Actinobacteria, Deferribacter, Firmicutes, BD1-5 and Verrucomicrobia were present in low numbers while Cyanobacteria were not observed in these samples. The contribution of Proteobacteria was highest in early December declining from near 90% of the total abundance to 61% while Bacteroidetes increased from 8 to near 30%. At the Class level, the Alphaproteobacteria was the most dominant group at all time points, followed by unassigned bacteria: Flavobacteria, Gammaproteobacteria and Sphingobacteria (Fig. 9). In contrast to the steady decrease in abundance observed in the Alphaproteobacteria, the Gammaproteobacteria nearly doubled their abundance towards the end of summer. Flavobacteria also doubled towards the end of summer, while Sphingobacteria (which were nearly absent in early summer) increased to 17% during mid-summer and declined to 9% at the end of summer. Actinobacteria also peaked during mid-summer (from 0.1% to nearly 1 %). In contrast, the unassigned group of Bacteria revealed a lowest abundance at mid-summer. At the order level, the SAR11 clade of the Alphaproteobacteria was the most abundant decreasing in relative contribution from 19 to 5% during the summer whereas the second most abundant order within the Alphaproteobacteria, the Rhodobacterales, increased from 2.8 to ~5.4% during summer. Among the Gammaproteobacteria, the Oceanospirillales were most abundant, steadily declining in relative abundance over time (from 3.2, 2.1 to 1.3%).

4. Discussion

Our study involved the first multi-primer approach to analyse microbial community changes as a function of Antarctic environmental conditions. Molecular fingerprinting methods such as DGGE have their limitations, such as over- or underestimating rRNA gene copy numbers which is further biased

when PCR is involved (Muyzer, 1999). There is a limit at which DGGE can successfully separate bands derived from different species and a potential for multiple bands belonging to one species, as discussed in Neilson et al. (2013). Yet even with the known pitfalls it has been successfully used to study microbial communities in polar regions (Díez et al., 2004; Gast et al., 2004; Ghiglione and Murray, 2012; Piquet et al., 2011, 2008). Current high-throughput DNA rRNA amplicon sequencing techniques could potentially analyse microbial communities at a higher resolution and identify organisms at or below the genus level depending on the gene or gene fragment of interest. However, such identification depends on coverage and annotation of the extant diversity, well-chosen primer sets and well maintained, curated databases for reference. The database is especially limited with regards to the oceanic micro-eukaryotes. In addition, shifts in the classical microscope-based phylogeny due to DNA based efforts further amplify the challenge of annotation to the species level (Medlin and Kaczmarska, 2004). Finally, species in extreme environments, such as ours, are often underrepresented in the reference databases. However, if supplemented with the classical taxon-specific pigment markers as proxies for phytoplankton group abundances, sequence results can give additional insights into ecologically relevant processes. For example, the pico-eukaryotes diversity and dynamics can now be studied more accurately (Yu et al., 2015).

4.1 Phytoplankton community dynamics

During spring, the observed dominance of haptophytes could have been due to deep mixing of the water column during the winter months (Montes-Hugo et al., 2009) in combination with the absence of sea ice (Rozema et al., 2016; Venables et al., 2013). Persistence of the winter/spring community was suggested to depend on the timing of water column freshening (Rozema et al., 2016). In contrast, diatoms dominated during summer as found earlier (Buma et al., 2001; Clarke et al., 2008; Garibotti et al., 2005; Luria et al., 2014; Piquet et al., 2011). Our finding that stratification mainly governs phytoplankton succession in northern Marguerite Bay is in general agreement with

earlier studies at the RaTS site (Piquet et al., 2011; Rozema et al., 2016). However, the influence of deviations from the expected N/P ratio adds a new perspective to phytoplankton community dynamics in northern Marguerite Bay.

After the first sampling date (December 9th), the observed increase in phytoplankton biomass coincided with enhanced meteoric water input. This increase was likely caused by pennate diatoms, which are more often associated with early season phytoplankton communities and sea-ice melting (period 1; Fig. 5 and 8; Annett et al., 2010; Ligowski et al., 1992; Pike et al., 2009). However, given the absence of sea ice in the period of investigation, it is not likely that the dominance of this group was derived from local sea-ice seeding. Increasing N/P ratios during this stage were possibly indicative of a mild limitation in micronutrients despite sufficient availability of macronutrients (Takeda, 1998). The wind-induced mixing event at the end of December and not a possible limitation in nutrients, was likely to end the period of phytoplankton growth (Bown et al., 2016). Despite this mixing, no shift towards P. antarctica (haptophytes as calculated by CHEMTAX (Fig. 5)) or cryptophytes was observed at 15 m. Apparently, relative diatom abundance was high enough to overcome short mixing events and prevented the establishment of groups more commonly associated with an unstable water column (Kozlowski et al ., 2011; Montes-Hugo et al., 2009; Rozema et al., 2016). This was further supported by size-fractionated Chl-a as phytoplankton consisted almost entirely of >20 μm cells until mid-January (Fig. 5).

The second period (Fig. 5) was characterized by a meltwater lens shallower than 5m (Fig. 2). The resultant strongly stratified water column could have stimulated biomass accumulation at 15 m. With 40% of the sequences (Table 2) allocated to the polar centrics, particularly belonging to the genus Thalassiosira, the phytoplankton community had changed significantly in contrast to the December sample. Thalassiosira species in this area were frequently observed and described in earlier studies (Annett et al., 2010; Garibotti et al., 2005; Piquet et al., 2011). The presence and high abundance of Thalassiosira genus was as expected given the global distribution and frequent observations in the coastal and open regions in the Southern Ocean (Armbrust, 2009; Díez et al., 2004; Ducklow et al.,

2012a; Pike et al., 2009; Piquet et al., 2008). As the MLD remained stable after the Chl-a peak, other factors must have caused the collapse of the bloom from January 17. While macronutrient concentrations were low, but not depleted (Fig. 4), N/P ratios decreased strongly (5.3 on January 27) after the peak in phytoplankton biomass. This decrease might suggest that low nitrogen availability prevented the persistence of the phytoplankton bloom. Yet, the NMDS analysis did not support this. Also, limitation by micronutrients or biomass loss due to grazing cannot be excluded (Behrenfeld, 2010; Bown et al., 2016).

During the third period (February 3-21) diatom dominated biomass increased to moderate levels. An increase in wind speed, and thus MLD, coincided with a strong decrease in salinity in the top 15 m due to meteoric water input (Fig. 3 and 5). Pennate diatoms underwent a relatively larger increase in relative abundance (0.72% to 4.03%) than polar centric diatoms (43.4% to 62.8%; Fig. 8), while radial centric diatoms decreased in relative contribution. Possibly, the continuously changing MLD, generally marking the end of summer, strongly shaped this changing community (Venables et al., 2013). There was no indication of limitation by nutrients, thus grazing or, more likely, light limitation prevented the build-up of large phytoplankton stocks.

4.2 Grazers and dinoflagellates

Sequencing results showed the presence of various grazers which were also reported in earlier microscopy and molecular (clone libraries) investigations of the eukaryotic community of Ryder Bay (Annett et al., 2010; Piquet et al., 2011) and Southern Ocean (Dolan et al., 2013; Georges et al., 2014). While half of the microplankton biomass in marine systems can consist of heterotrophic dinoflagellates (Sherr and Sherr, 2007), early efforts using pyrosequencing showed that most of the sequences north of the Polar Front were derived from dinoflagellates. South of the Polar Front they decreased in observed frequency and contributed ~30% to the total number of reads (Wolf et al., 2013). In our study dinoflagellate-related pigments were hardly observed throughout the summer

season. Possibly, Antarctic dinoflagellates were underestimated by CHEMTAX as many species might have been categorized as haptophytes. Yet, as haptophytes abundances during summer were low, a potentially mislabelled dinoflagellate component would not alter our conclusions on relative phytoplankton abundances significantly (Fig. 5). In contrast, we found 20 to 35% of our eukaryote sequences to be assigned to dinoflagellates. This discrepancy suggests a dominance of heterotrophic dinoflagellates with only a minor contribution of autotrophs. However we have to keep in mind abundance estimates based on sequences are not easily translated to multicellular organisms or organisms with high copy numbers of the gene used for barcoding, such as dinoflagellates (Zhu et al., 2005). As a result, an overestimation of dinoflagellate abundance based on sequence data is possible. Annett et al. (2010) found that dinoflagellates (auto- and heterotrophic) abundances were low in Ryder Bay. Yet, given the large size of some species and relative high C content they could still contribute significantly to microbial biomass. Therefore, detailed studies on dinoflagellate dynamics might benefit from a combination of chemotaxonomic, microscopic and molecular approaches.

4.3 Bacterial community

Community fingerprints of samples collected on December 9 and January 13 clustered and these bacteria most likely originated from the winter/spring community (Fig. 7). The later January (24 and 27) samples appear to have responded to the peak in Chl-a in period 1, while the bacterial samples collected thereafter indicated a response of the bacterial community to the seasonal high in Chl-a during period 2. The February 21 sample was similar to the previous cluster (Jan 31 – Feb 16) mimicking the high similarity between succession in the photosynthetic community, albeit with a delay. The bacterial communities frequently correspond with a lag-phase to phytoplankton biomass and composition (Ghiglione and Murray, 2012; Piquet et al., 2011). The bacterial community in the BAC3 clustered appeared to have played a pivotal role in remineralizing major nutrients as these were increasing despite increasing phytoplankton biomass (Landa et al., 2016). This source of

nutrients replenishment, in combination with vertical mixing, presumably allowed for renewed phytoplankton growth after a large bloom. Based on our UPGMA results (grouping of January 13 in BAC and EUK clusters) we estimated a lag phase between phytoplankton peak in Chl-a and bacterial response of 1 to 2 weeks, however, care must be taken given the limited data set. Moran et al., (2001) showed that bacterial production was coupled to recently produced DOC by algae and thus related to primary production. Ducklow et al. (2012b) also showed the coupling between Bacteria and phytoplankton based on correlations between leucine incorporation rates and both primary production and Chl-a. That study showed a stronger correlation between bacterial biomass and Chl-a than with primary production which confirms our finding of Chl-a concentration being important in bacterial community composition (Fig. 7). Our data are supported by earlier findings of Piquet et al. (2011), where the bacterial community was found be influenced by the factors that also shaped the eukaryotic community, in particular stratification and mixing, although Chl-a was excluded in the previous study.

Alphaproteobacteria and Bacteroidetes dominance (Fig. 9) is in agreement with other studies that confirm their ubiquitous presence in the Southern Ocean and Antarctic coastal sites (Gentile et al., 2006; Ghiglione and Murray, 2012; Luria et al., 2014; Piquet et al., 2011; Straza et al., 2010). Alphaproteobacteria, especially the ubiquitous SAR11 clade were abundant in mid-December in our study. The low light conditions during the transition between Antarctic summer and winter may favour the photoheterotrophic SAR11 group over other bacterial groups. In contrast, during late spring and summer they would be outcompeted for light by eukaryotic phytoplankton (Ducklow et al., 2007; Grzymski et al., 2012; Williams et al., 2012). In addition, relative haptophyte abundance was high after the winter and thus surface waters could be enriched with dissolved low molecular weight compounds such as DMSP. Previous observations have coupled the metabolically diverse generalists of the alphaproteobacterial class with decaying algal blooms releasing dissolved low molecular weight compounds such as DMSP (Curson et al., 2008; Malmstrom et al., 2004; Reisch et al., 2011). The initial abundance of Alphaproteobacteria could be related to the release of low

molecular weight carbon sources by haptophytes which is followed by a later response of the Bacteroidetes to diatom dominance in summer. Bacteroidetes relative abundance increased after two periods of high Chl-a dominated by diatoms at the end December and in January (periods 1 & 2; Fig. 5). A proposed preference of Bacteroidetes species for high molecular weight carbon compounds was recently confirmed by genomic analysis of several Bacteroidetes strains (Fernández-Gómez et al., 2013). This might also explain why Actinobacteria, also specialized in the degradation of high molecular weight carbon, displayed a similar trend as the Bacteroidetes.

4.4 Group specific variability

Variability in response times differed between the various groups of microorganism studies here. Not only did we observe a lag phase in the response of the bacteria when confronted with a changing phytoplankton community after the collapse of a bloom but also between different eukaryotic groups. The trends observed for the general eukaryotes were different than those of the diatoms and dinoflagellates (Fig. 6 & 7) while more similarity was initially expected. Variability in these latter two groups was less than observed in the general eukaryotes (Table 1). A possible explanation might be related to the choice of methodology. DGGE (and PCR) is a good, frequently-used technique for describing species represented by more than ~1% of the environmental DNA. Thus, a particular portion of the ecosystem was described when using primers for general eukaryotes as this includes grazers, dinoflagellates, diatoms, and many other groups varying in amounts of DNA. To be present in the DNA the species need to have a large copy number of the gene or be highly abundant ("blooming"). The specific primers for diatoms and dinoflagellates are more likely to include "all" species present, including those with at low abundance (<~1%). The low abundance species might have been missed by the general eukaryote primers. As such, responses to environmental conditions of the specific groups will be less clear as the capabilities of DGGE for quantitative analysis are mediocre. Thus, we conclude that the eukaryotic community changes, from picophytoplankton to

large grazers, respond to larger environmental shifts. The decreased variability in the specific groups illustrates the plasticity of the eukaryotic microbial community improving resilience of the ecosystem in an extreme environment (Barton et al., 2010).

4.5 Current and future implications

Our hypothesis that phytoplankton succession is governed by periods of enhanced water column stability was confirmed by our study. It is well established that meltwater input affects Antarctic phytoplankton biomass accumulation through the increase in stratification, consequential alteration of the light and mixing regime and potential iron enrichment (Alderkamp et al., 2012; Dierssen et al., 2002; Gerringa et al., 2012; Saba et al., 2014). Furthermore, as hypothesized, limitation by macronutrients was not observed. Finally, as hypothesized, the bacterial community showed a delayed response to shifts in phytoplankton community composition. The summer of 2010-2011 investigated in the present study was relatively warm compared with previous years, and characterized by the absence of sea-ice cover and high meteoric water input, inferred to be predominantly from glacial origin. These conditions clearly led to a diatom dominated phytoplankton assemblage throughout the summer. In contrast, years characterized by low phytoplankton biomass were found to be dominated by P. antarctica and/or cryptophytes, most likely resulting from an unstable water column due to the absence of sea ice in the preceding winter (Rozema et al., 2016). Our study represented what appeared to be a typical Antarctic summer with average levels of phytoplankton biomass (Rozema et al., 2016). The discussed dynamics might be different in summers when relative diatom contributions and phytoplankton biomass are low.

The future climatic evolution of the WAP is not easy to predict, however further increases in glacial discharge are likely (Cook et al., 2016). As a result shifts in the phytoplankton community might occur, such as a decrease in average phytoplankton size (Moline et al., 2004; Montes-Hugo et al., 2009; Saba et al., 2014). This shift in size classes might be due to a decrease in diatoms and an

increase in cryptophytes and/or haptophytes (Arrigo et al., 1999; Moline et al., 2004; Rozema et al., 2016; Saba et al., 2014). Yet, despite a steady increase of glacial meltwater, increased cryptophyte abundances during summer stratification were not observed in our study, at least not at the depth of our interest where glacial influences were still observed (Fig. 3 and 5; Table 2). Depth resolved variability in microbial community composition at the RaTS was studied during more recent summer seasons. The shift from diatoms to cryptophytes could affect the bacterial community and important consumers such as krill, since krill prefers diatoms as their primary food source (Haberman et al., 2003). Krill forms the main trophic link to higher levels within the Antarctic food web (Atkinson et al., 2004; Trivelpiece et al., 2011). Thus, changes in the phytoplankton community could affect the entire Antarctic food web. We have shown that the reduction of MLD during summer, as caused by meltwater-related surface stratification, promotes a succession in diatoms rather than (nano)phytoflagellates in northern Marguerite Bay. This might favour higher trophic levels, in particular after relatively warm winters with low sea-ice cover, where phytoplankton dynamics could otherwise be characterised by lower biomass throughout and the dominance of less-edible phytoflagellate groups (Haberman et al., 2003; Saba et al., 2014).

5. Acknowledgements

We would like to thank the Marine Assistants and other staff at Rothera and in Cambridge who have contributed to the collection of the samples and data used here. Also, we thank Ronald Visser for his assistance with HPLC analyses. Corina Brussaard is thanked for a valued discussion of an early draft of the manuscript. Finally, we would like to thank the editors, Simon Wright and two anonymous reviewers for their insights and helpful suggestions on improving this paper. This research was funded by the Dutch Polar Programme (866.10.105). Funding for the RaTS programme is from the Natural Environment Research Council, and is a component of the BAS Polar Oceans programme.

References

Abell, G.C.J., Bowman, J.P., 2005. Ecological and biogeographic relationships of class Flavobacteria in the Southern Ocean. FEMS Microbiol. Ecol. 51, 265–277. doi:10.1016/j.femsec.2004.09.001

Ackley, S.F., Sullivan, C.W., 1994. Physical controls on the development and characteristics of Antarctic sea-ice biological bommunities - a review and synthesis. Deep. Res. Part I Oceanogr. Res. Pap. 41, 1583–1604. doi:10.1016/0967-0637(94)90062-0

Alderkamp, A.-C., Mills, M.M., van Dijken, G.L., Laan, P., Thuróczy, C.E., Gerringa, L.J.A., de Baar, H.J.W., Payne, C.D., Visser, R.J.W., Buma, A.G.J., Arrigo, K.R., 2012. Iron from melting glaciers fuels phytoplankton blooms in the Amundsen Sea (Southern Ocean): Phytoplankton characteristics and productivity. Deep. Res. Part II Top. Stud. Oceanogr. 71–76, 32–48. doi:10.1016/j.dsr2.2012.03.005

Amann, R.I., Binder, B.J., Olson, R.J., Chisholm, S.W., Devereux, R., Stahl, D.A., 1990. Combination of 16S rRNA-targeted oligonucleotide probes with flow cytometry for analyzing mixed microbial populations. Appl. Environ. Microbiol. 56, 1919–1925. doi:10.1111/j.1469-8137.2004.01066.x

Annett, A.L., Carson, D.S., Crosta, X., Clarke, A., Ganeshram, R.S., 2010. Seasonal progression of diatom assemblages in surface waters of Ryder Bay, Antarctica. Polar Biol. 33, 13–29. doi:10.1007/s00300-009-0681-7

Armbrust, E.V., 2009. The life of diatoms in the world's oceans. Nature 459, 185–192.

Arrigo, K.R., Robinson, D.H., Worthen, D.L., Dunbar, R.B., DiTullio, G.R., VanWoert, M., Lizotte, M.P., 1999. Phytoplankton community structure and the drawdown of nutrients and CO2 in the Southern Ocean. Science (80). 283, 365–367. doi:10.1126/science.283.5400.365

Atkinson, A., Siegel, V., Pakhomov, E., Rothery, P., 2004. Long-term decline in krill stock and increase in salps within the Southern Ocean. Nature 432, 100–103. doi:10.1038/nature02996

Atkinson, A., Ward, P., Hunt, B.P. V, Pakhomov, E.A., Hosie, G.W., 2012. An overview of Southern Ocean zooplankton data: Abundance, biomass, feeding and functional relationships. CCAMLR Sci. 19, 171–218.

Barton, A.D., Dutkiewicz, S., Flierl, G., Bragg, J., Follows, M.J., 2010. Patterns of Diversity in Marine Phytoplankton. Science (80-.). 327, 1509–1511. doi:10.1126/science.1184961

Behrenfeld, M.J., 2010. Abandoning Sverdrup's Critical Depth Hypothesis on phytoplankton blooms Critical Depth Hypothesis Abandoning Sverdrup ' s on phytoplankton. Ecology 91, 977–989. doi:10.1890/09-1207.1

Billen, G., Becquevort, S., 1991. Phytoplankton Bacteria relationship in the Antarctic marine ecosystem. Polar Res. 10, 245–253.

Boelen, P., De Boer, M.K., Kraay, G.W., Veldhuis, M.J.W., Buma, A.G.J., 2000. UVBR-induced DNA damage in natural marine picoplankton assemblages in the tropical Atlantic Ocean. Mar. Ecol. Prog. Ser. 193, 1–9. doi:10.3354/meps193001

Bown, J., Laan, P., Ossebaar, S., Bakker, K., Rozema, P.D., de Baar, H.J.W., Baar, H.J.W. De, 2016. Bioactive trace metal time series during Austral summer in Ryder Bay, Western Antarctic Peninsula. Deep Sea Res. Part II Top. Stud. Oceanogr. 1–17. doi:10.1016/j.dsr2.2016.07.004

Brainerd, K.E., Gregg, M.C., 1995. Surface mixed and mixing layer depths. Deep. Res. Part I Oceanogr. Res. Pap. 42, 1521–1543. doi:10.1016/0967-0637(95)00068-H

Buma, A.G.J., de Boer, M.K., Boelen, P., 2001. Depth distributions of DNA damage in antarctic marine phyto and bacterioplankton exposed to summertime UV radiation. J. Phycol. 37, 200–208. doi:10.1046/j.1529-8817.2001.037002200.x

Caporaso, J.G., Kuczynski, J., Stombaugh, J., Bittinger, K., Bushman, F.D., Costello, E.K., Fierer, N., Peña, A.G., Goodrich, J.K., Gordon, J.I., Huttley, G. a, Kelley, S.T., Knights, D., Koenig, J.E., Ley, R.E., Lozupone, C. a, McDonald, D., Muegge, B.D., Pirrung, M., Reeder, J., Sevinsky, J.R., Turnbaugh, P.J., Walters, W. a, Widmann, J., Yatsunenko, T., Zaneveld, J., Knight, R., 2010.

QIIME allows analysis of high-throughput community sequencing data. Nat. Methods 7, 335–336. doi:10.1038/nmeth.f.303

Clarke, A., Meredith, M.P., Wallace, M.I., Brandon, M.A., Thomas, D.N., 2008. Seasonal and interannual variability in temperature, chlorophyll and macronutrients in northern Marguerite Bay, Antarctica. Deep. Res. Part II Top. Stud. Oceanogr. 55, 1988–2006. doi:10.1016/j.dsr2.2008.04.035

Cook, A.J., Fox, A.J., Vaughan, D.G., Ferrigno, J.G., 2005. Retreating glacier fronts on the Antarctic Peninsula over the past half-century. Science (80-.). 308, 541–544. doi:10.1126/science.1104235

Cook, A.J., Holland, P.R., Meredith, M.P., Murray, T., Luckman, A., Vaughan, D.G., 2016. Ocean forcing of glacier retreat in the western Antarctic Peninsula. Science (80-.). 353, 283–286. doi:10.1126/science.aae0017

Craig, H., Gordon, L., 1965. Deuterium and Oxygen-18 Variations In the Ocean and The Marine Atmosphere., in: Tongiorgio, E. (Ed.), Proceedings of a Conference On Stable Isotopes In Oceanographic Studies and Paleotemperatures. Spoleto, Italy, pp. 9–130.

Curson, A.R.J., Rogers, R., Todd, J.D., Brearley, C.A., Johnston, A.W.B., 2008. Molecular genetic analysis of a dimethylsulfoniopropionate lyase that liberates the climate-changing gas dimethylsulfide in several marine alpha-proteobacteria and Rhodobacter sphaeroides. Environ. Microbiol. 10, 757–67. doi:10.1111/j.1462-2920.2007.01499.x

Delmont, T.O., Hammar, K.M., Ducklow, H.W., Yager, P.L., Post, A.F., 2014. Phaeocystis antarctica blooms strongly influence bacterial community structures in the Amundsen Sea polynya. Front. Microbiol. 5. doi:10.3389/fmicb.2014.00646

Depoorter, M.A., Bamber, J.L., Griggs, J.A., Lenaerts, J.T.M., Ligtenberg, S.R.M., van den Broeke, M.R., Moholdt, G., 2013. Calving fluxes and basal melt rates of Antarctic ice shelves. Nature 502, 89–92. doi:10.1038/nature12567

Dierssen, H.M., Smith, R.C., Vernet, M., 2002. Glacial meltwater dynamics in coastal waters west of the Antarctic peninsula. Proc. Natl. Acad. Sci. U. S. A. 99, 1790–1795. doi:DOI 10.1073/pnas.032206999

Díez, B., Massana, R., Estrada, M., Pedrós-Alió, C., 2004. Distribution of eukaryotic picoplankton assemblages across hydrographic fronts in the Southern Ocean, studied by denaturing gradient gel electrophoresis. Limnol. Oceanogr. 49, 1022–1034. doi:10.4319/lo.2004.49.4.1022

Díez, B., Pedrós-Alió, C., Marsh, T.L., Pedro, C., 2001. Application of Denaturing Gradient Gel Electrophoresis (DGGE) to study the diversity of marine picoeukaryotic assemblages and comparison of DGGE with other molecular techniques. Appl. Environ. Microbiol. 67, 2942–2951. doi:10.1128/AEM.67.7.2942

Dolan, J.R., Yang, E.J., Lee, S.H., Kim, S.Y., 2013. Tintinnid ciliates of amundsen sea (Antarctica) plankton communities. Polar Res. 32, 1–12. doi:10.3402/polar.v32i0.19784

Ducklow, H.W., Baker, K., Martinson, D.G., Quetin, L.B., Ross, R.M., Smith, R.C., Stammerjohn, S.E., Vernet, M., Fraser, W., 2007. Marine pelagic ecosystems: the west Antarctic Peninsula. Philos. Trans. R. Soc. Lond. B. Biol. Sci. 362, 67–94. doi:10.1098/rstb.2006.1955

Ducklow, H.W., Clarke, A., Dickhut, R., Doney, S.C., Geisz, H., Kuan Huang, Martinson, D.G., Schofield, O.M.E., Stammerjohn, S.E., Steinberg, D.K., Fraser, W.R., 2012a. The Marine System of the Western Antarctic Peninsula. Antarct. Ecosyst. An Extrem. Environ. a Chang. World 121–159.

Ducklow, H.W., Schofield, O., Vernet, M., Stammerjohn, S., Erickson, M., 2012b. Multiscale control of bacterial production by phytoplankton dynamics and sea ice along the western Antarctic Peninsula: A regional and decadal investigation. J. Mar. Syst. 98–99, 26–39. doi:10.1016/j.jmarsys.2012.03.003

Fernández-Gómez, B., Richter, M., Schüler, M., Pinhassi, J., Acinas, S.G., González, J.M., Pedrós-Alió, C., 2013. Ecology of marine Bacteroidetes: a comparative genomics approach. ISME J. 7, 1026–37. doi:10.1038/ismej.2012.169

Flores, H., Atkinson, A., Kawaguchi, S., Krafft, B. a., Milinevsky, G., Nicol, S., Reiss, C., Tarling, G. a., Werner, R., Bravo Rebolledo, E., Cirelli, V., Cuzin-Roudy, J., Fielding, S., Groeneveld, J.J., Haraldsson, M., Lombana, A., Marschoff, E., Meyer, B., Pakhomov, E. a., Rombolá, E., Schmidt, K., Siegel, V., Teschke, M., Tonkes, H., Toullec, J.Y., Trathan, P.N., Tremblay, N., Van de Putte, A., van Franeker, J. a., Werner, T., 2012. Impact of climate change on Antarctic krill. Mar. Ecol. Prog. Ser. 458, 1–19. doi:10.3354/meps09831

Frank, K.L., Rogers, D.R., Olins, H.C., Vidoudez, C., Girguis, P.R., 2013. Characterizing the distribution and rates of microbial sulfate reduction at Middle Valley hydrothermal vents. ISME J. 7, 1391–401. doi:10.1038/ismej.2013.17

Garibotti, I.A., Vernet, M., Ferrario, M.E., 2005. Annually recurrent phytoplanktonic assemblages during summer in the seasonal ice zone west of the Antarctic Peninsula (Southern Ocean). Deep. Res. Part I Oceanogr. Res. Pap. 52, 1823–1841. doi:10.1016/j.dsr.2005.05.003

Gast, R.J., Dennett, M.R., Caron, D. a., 2004. Characterization of Protistan Assemblages in the Ross Sea, Antarctica, by Denaturing Gradient Gel Electrophoresis. Appl. Environ. Microbiol. 70, 2028–2037. doi:10.1128/AEM.70.4.2028–2037.2004

Gentile, G., Giuliano, L., D'Auria, G., Smedile, F., Azzaro, M., De Domenico, M., Yakimov, M.M., 2006. Study of bacterial communities in Antarctic coastal waters by a combination of 16S rRNA and 16S rDNA sequencing. Environ. Microbiol. 8, 2150–2161. doi:10.1111/j.1462-2920.2006.01097.x

Georges, C., Monchy, S., Genitsaris, S., Christaki, U., 2014. Protist community composition during early phytoplankton blooms in the naturally iron-fertilized Kerguelen area (Southern Ocean). Biogeosciences 11, 5847–5863. doi:10.5194/bg-11-5847-2014

Gerringa, L.J.A., Alderkamp, A.-C., Laan, P., Thuróczy, C.-E., De Baar, H.J.W., Mills, M.M., van Dijken, G.L., Haren, H. van, Arrigo, K.R., 2012. Iron from melting glaciers fuels the phytoplankton blooms in Amundsen Sea (Southern Ocean): Iron biogeochemistry. Deep. Res. Part II Top. Stud. Oceanogr. 71–76, 16–31. doi:10.1016/j.dsr2.2012.03.007

Ghiglione, J.F., Murray, A.E., 2012. Pronounced summer to winter differences and higher wintertime richness in coastal Antarctic marine bacterioplankton. Environ. Microbiol. 14, 617–629. doi:10.1111/j.1462-2920.2011.02601.x

Giovannoni, S.J., DeLong, E.F., Olsen, G.J., Pace, N.R., 1988. Phylogenetic group-specific oligodeoxynucleotide probes for identification of single microbial cells. J. Bacteriol. 170, 720–726.

Godhe, A., Asplund, M.E., Härnström, K., Saravanan, V., Tyagi, A., Karunasagar, I., 2008. Quantification of diatom and dinoflagellate biomasses in coastal marine seawater samples by real-time PCR. Appl. Environ. Microbiol. 74, 7174–7182. doi:10.1128/AEM.01298-08

Grzymski, J.J., Riesenfeld, C.S., Williams, T.J., Dussaq, A.M., Ducklow, H., Erickson, M., Cavicchioli, R., Murray, A.E., 2012. A metagenomic assessment of winter and summer bacterioplankton from Antarctica Peninsula coastal surface waters. ISME J. 6, 1901–1915. doi:10.1038/ismej.2012.31

Haberman, K.L., Ross, R.M., Quetin, L.B., 2003. Diet of the Antarctic krill (Euphausia superba Dana): II. Selective grazing in mixed phytoplankton assemblages. J. Exp. Mar. Bio. Ecol. 283, 97–113. doi:10.1016/S0022-0981(02)00467-7

Hammer, Ø., Harper, D.A.T., Ryan, P.D., 2001. PAST: Palaeontological statistics software package for education and data analysis. Palaeontol. Electron. 4, 1–9. doi:10.1163/001121611X566785

Heuer, H., Wieland, G., Schonfeld, J., Schonwalder, A., Gomes, N.C.M., Smalla, K., 2001. Bacterial community profiling using DGGE or TGGE analysis, Environmental molecular microbiology: Protocols and applications. Horizon Scientific Press, Wymondham.

Kim, J.G., Park, S.J., Quan, Z.X., Jung, M.Y., Cha, I.T., Kim, S.J., Kim, K.H., Yang, E.J., Kim, Y.N., Lee, S.H., Rhee, S.K., 2014. Unveiling abundance and distribution of planktonic Bacteria and Archaea in a polynya in Amundsen Sea, Antarctica. Environ. Microbiol. 16, 1566–1578. doi:10.1111/1462-2920.12287

Kozlowski, W.A., Deutschman, D., Garibotti, I., Trees, C., Vernet, M., 2011. An evaluation of the

application of CHEMTAX to Antarctic coastal pigment data. Deep. Res. Part I Oceanogr. Res. Pap. 58, 350–364. doi:10.1016/j.dsr.2011.01.008

Ladau, J., Sharpton, T.J., Finucane, M.M., Jospin, G., Kembel, S.W., O'Dwyer, J., Koeppel, A.F., Green, J.L., Pollard, K.S., 2013. Global marine bacterial diversity peaks at high latitudes in winter. ISME J. 7, 1669–1677. doi:10.1038/ismej.2013.37

Landa, M., Blain, S., Christaki, U., 2016. Shifts in bacterial community composition associated with increased carbon cycling in a mosaic of phytoplankton blooms. ISME J. 10, 39.50. doi:10.1038/ismej.2015.105

Ligowski, R., Godlewski, M., Lukowski, A., 1992. Sea ice diatoms and ice edge planktonic diatoms at the northern limit of the Weddell Sea pack ice. Proc. NIPR Symp. Polar Biol. 5, 9–20.

Lin, S., Zhang, H., Hou, Y., Miranda, L., Bhattacharya, D., 2006. Development of a dinoflagellate-oriented PCR primer set leads to detection of picoplanktonic dinoflagellates from Long Island Sound. Appl. Environ. Microbiol. 72, 5626–30. doi:10.1128/AEM.00586-06

Luria, C., Ducklow, H., Amaral-Zettler, L., 2014. Marine bacterial, archaeal and eukaryotic diversity and community structure on the continental shelf of the western Antarctic Peninsula. Aquat. Microb. Ecol. 73, 107–121. doi:10.3354/ame01703

Mackey, M.D., Mackey, D.J., Higgins, H.W., Wright, S.W., 1996. CHEMTAX - A program for estimating class abundances from chemical markers: Application to HPLC measurements of phytoplankton. Mar. Ecol. Prog. Ser. 144, 265–283. doi:10.3354/meps144265

Malmstrom, R.R., Kiene, R.P., Cottrell, M.T., Kirchman, D.L., 2004. Contribution of SAR11 bacteria to dissolved dimethylsulfoniopropionate and amino acid uptake in the North Atlantic Ocean. Appl. Environ. Microbiol. 70, 4129–4135. doi:10.1128/AEM.70.7.4129-4135.2004

Medlin, L., Elwood, H.J., Stickel, S., Sogin, M.L., 1988. The characterization of enzymatically amplified eukaryotic 16S-like rRNA-coding regions. Gene 71, 491–499. doi:10.1016/0378-1119(88)90066-2

Medlin, L.K., Kaczmarska, I., 2004. Evolution of the diatoms: V. Morphological and cytological support for the major clades and a taxonomic revision. Phycologia 43, 245–270. doi:10.2216/i0031-8884-43-3-245.1

Meredith, M.P., Brandon, M.A., Wallace, M.I., Clarke, A., Leng, M.J., Renfrew, I.A., van Lipzig, N.P.M., King, J.C., 2008. Variability in the freshwater balance of northern Marguerite Bay, Antarctic Peninsula: Results from delta O-18. Deep. Res. Part II Top. Stud. Oceanogr. 55, 309–322. doi:10.1016/j.dsr2.2007.11.005

Meredith, M.P., Stammerjohn, S.E., Venables, H.J., Ducklow, H.W., Martinson, D.G., Iannuzzi, R.A., Leng, M.J., van Wessem, J.M., Reijmer, C.H., Barrand, N.E., 2016. Changing distributions of sea ice melt and meteoric water west of the Antarctic Peninsula. Deep. Res. Part II Top. Stud. Oceanogr. 1–18. doi:10.1016/j.dsr2.2016.04.019

Meredith, M.P., Venables, H.J., Clarke, A., Ducklow, H.W., Erickson, M., Leng, M.J., Lenaerts, J.T.M.M., van den Broeke, M.R., 2013. The freshwater system west of the Antarctic Peninsula: spatial and temporal changes. J. Clim. 26, 1669–1684. doi:10.1175/JCLI-D-12-00246.1

Meredith, M.P., Wallace, M.I., Stammerjohn, S.E., Renfrew, I. a., Clarke, A., Venables, H.J., Shoosmith, D.R., Souster, T., Leng, M.J., 2010. Changes in the freshwater composition of the upper ocean west of the Antarctic Peninsula during the first decade of the 21st century. Prog. Oceanogr. 87, 127–143. doi:10.1016/j.pocean.2010.09.019

Moline, M.A., Claustre, H., Frazer, T.K., Schofield, O., Vernet, M., 2004. Alteration of the food web along the Antarctic Peninsula in response to a regional warming trend. Glob. Chang. Biol. 10, 1973–1980. doi:10.1111/j.1365-2486.2004.00825.x

Montes-Hugo, M., Doney, S.C., Ducklow, H.W., Fraser, W.R., Martinson, D., Stammerjohn, S.E., Schofield, O., 2009. Recent changes in phytoplankton communities associated with rapid regional climate change along the western Antarctic Peninsula. Science (80-.). 323, 1470–1473. doi:10.1126/science.1164533

Moran, X.A.G., Gasol, J.M., Estrada, M., Pedros-Alio, C., 2001. Dissolved and particulate primary production and bacterial production in offshore antarctic waters during austral summer:coupled or uncoupled? Mar. Ecol. Prog. Ser. 222, 25–39.

Moreno, A.M., Matz, C., Kjelleberg, S., Manefield, M., 2010. Identification of ciliate grazers of autotrophic bacteria in ammonia-oxidizing activated sludge by RNA stable isotope probing. Appl. Environ. Microbiol. 76, 2203–2211. doi:10.1128/AEM.02777-09

Muyzer, G., 1999. DGGE / TGGE a method natural ecosystems for identifying genes from natural ecosystems. Curr. Opin. Microbiol. 2, 317–322. doi:10.1016/S1369-5274(99)80055-1

Neilson, J.W., Jordan, F.L., Maier, R.M., 2013. Analysis of Artifacts Suggests DGGE Should Not Be Used For Quantitative Diversity Analysis. J. Microbiol. Methods 92, 256–263. doi:10.1016/j.mimet.2012.12.021

Nübel, U., Engelen, B., Felske, A., Snaidr, J., Wieshuber, A., Amann, R.I., Ludwig, W., Backhaus, H., Engelen, B., Felske, A., Snaidr, J., Wieshuber, A., 1996. Sequence heterogeneities of genes encoding 16S rRNAs in Paenibacillus polymyxa detected by temperature gradient gel electrophoresis. J. Bacteriol. 178, 5636–5643.

Peck, L.S., Barnes, D.K.A., Cook, A.J., Fleming, A.H., Clarke, A., 2010. Negative feedback in the cold: Ice retreat produces new carbon sinks in Antarctica. Glob. Chang. Biol. 16, 2614–2623. doi:10.1111/j.1365-2486.2009.02071.x

Perl, J., 2009. The SDU (CHORS) Method, in: The Third SeaWiFS HPLC Analysis Round-Robin Experiment (SeaHARRE-3). NASA, pp. 89–91.

Pike, J., Crosta, X., Maddison, E.J., Stickley, C.E., Denis, D., Barbara, L., Renssen, H., 2009. Observations on the relationship between the Antarctic coastal diatoms Thalassiosira antarctica Comber and Porosira glacialis (Grunow) Jørgensen and sea ice concentrations during the late Quaternary. Mar. Micropaleontol. 73, 14–25. doi:http://dx.doi.org/10.1016/j.marmicro.2009.06.005

Piquet, A.M.T., Bolhuis, H., Davidson, A.T., Thomson, P.G., Buma, a. G.J., 2008. Diversity and dynamics of Antarctic marine microbial eukaryotes under manipulated environmental UV radiation. FEMS Microbiol. Ecol. 66, 352–366. doi:10.1111/j.1574-6941.2008.00588.x

Piquet, A.M.T., Bolhuis, H., Meredith, M.P., Buma, A.G.J., 2011. Shifts in coastal Antarctic marine microbial communities during and after melt water-related surface stratification. FEMS Microbiol. Ecol. 76, 413–427. doi:10.1111/j.1574-6941.2011.01062.x

Piquet, A.M.T., van de Poll, W.H., Visser, R.J.W., Wiencke, C., Bolhuis, H., Buma, A.G.J., 2014. Springtime phytoplankton dynamics in Arctic Krossfjorden and Kongsfjorden (Spitsbergen) as a function of glacier proximity. Biogeosciences 11, 2263–2279. doi:10.5194/bg-11-2263-2014

Quast, C., Pruesse, E., Yilmaz, P., Gerken, J., Schweer, T., Yarza, P., Peplies, J., Glöckner, F.O., 2013. The SILVA ribosomal RNA gene database project: Improved data processing and web-based tools. Nucleic Acids Res. 41, 590–596. doi:10.1093/nar/gks1219

Quetin, L.B., Ross, R.M., 1985. Feeding by Antarctic krill, Euphausia superba: does size matter? Antarct. Nutr. Cycles Food Webs.

Ramette, A., 2007. Multivariate analyses in microbial ecology. FEMS Microbiol. Ecol. 62, 142–60. doi:10.1111/j.1574-6941.2007.00375.x

Redfield, A.C., 1958. The biological control of chemical factors in the environment. Am. Sci. 46, 205–221.

Reisch, C.R., Moran, M.A., Whitman, W.B., 2011. Bacterial Catabolism of Dimethylsulfoniopropionate (DMSP). Front. Microbiol. 2, 172. doi:10.3389/fmicb.2011.00172

Rignot, E., Jacobs, S., Mouginot, J., Scheuchl, B., 2013. Ice-shelf melting around Antarctica. Science (80-.). 341, 266–70. doi:10.1126/science.1235798

Rozema, P.D., Venables, H.J., van de Poll, W.H., Clarke, A., Meredith, M.P., Buma, A.G.J., 2016. Interannual variability in phytoplankton biomass and species composition in northern

Marguerite Bay (West Antarctic Peninsula) is governed by both winter sea ice cover and summer stratification. Limnol. Oceanogr. doi:10.1002/lno.10391

Saba, G.K., Fraser, W.R., Saba, V.S., Iannuzzi, R. a, Coleman, K.E., Doney, S.C., Ducklow, H.W., Martinson, D.G., Miles, T.N., Patterson-Fraser, D.L., Stammerjohn, S.E., Steinberg, D.K., Schofield, O.M., 2014. Winter and spring controls on the summer food web of the coastal West Antarctic Peninsula. Nat. Commun. 5, 4318. doi:10.1038/ncomms5318

Schlitzer, R., 2013. Ocean Data View [WWW Document].

Sherr, E.B., Sherr, B.F., 2007. Heterotrophic dinoflagellates: A significant component of microzooplankton biomass and major grazers of diatoms in the sea. Mar. Ecol. Prog. Ser. doi:10.3354/meps07161

Simpson, E.H., 1949. Measurement of diversity. Nature 163, 688. doi:10.1038/163688a0

Sogin, M.L., Gunderson, J.H., 1987. Structural diversity of eukaryotic small subunit ribosomal RNAs. Evolutionary implications. Ann. N. Y. Acad. Sci. 503, 125–139.

Steig, E.J., Schneider, D.P., Rutherford, S.D., Mann, M.E., Comiso, J.C., Shindell, D.T., 2009. Warming of the Antarctic ice-sheet surface since the 1957 International Geophysical Year. Nature 457, 459–462. doi:10.1038/nature08286

Steinberg, D.K., Ruck, K.E., Gleiber, M.R., Garzio, L.M., Cope, J.S., Bernard, K.S., Stammerjohn, S.E., Schofield, O.M.E., Quetin, L.B., Ross, R.M., 2015. Long-term (1993-2013) changes in macrozooplankton off the western antarctic peninsula. Deep. Res. Part I Oceanogr. Res. Pap. 101, 54–70. doi:10.1016/j.dsr.2015.02.009

Straza, T.R. a., Ducklow, H.W., Murray, A.E., Kirchman, D.L., 2010. Abundance and single-cell activity of bacterial groups in Antarctic coastal waters. Limnol. Oceanogr. 55, 2526–2536. doi:10.4319/lo.2010.55.6.2526

Sverdrup, H., 1953. On conditions for the vernal blooming of phytoplankton. J. du Cons. 18, 287–295.

doi:10.4319/lom.2007.5.269

Takeda, S., 1998. Influence of iron availability on nutrient consumption ratio of diatoms in oceanic waters. Nature 393, 774–777. doi:10.1038/31674

Torbjørn, R., 2015. Vsearch: VSEARCH version 1.1.3. Zenodo. [WWW Document]. doi:10.5281/zenodo.16153

Trivelpiece, W.Z., Hinke, J.T., Miller, A.K., Reiss, C.S., Trivelpiece, S.G., Watters, G.M., 2011. Variability in krill biomass links harvesting and climate warming to penguin population changes in Antarctica. Proc. Natl. Acad. Sci. U. S. A. 108, 7625–7628. doi:10.1073/pnas.1016560108

Turner, J., Colwell, S.R., Marshall, G.J., Lachlan-Cope, T. a., Carleton, A.M., Jones, P.D., Lagun, V., Reid, P. a., Iagovkina, S., 2005. Antarctic climate change during the last 50 years. Int. J. Climatol. 25, 279–294. doi:10.1002/joc.1130

Turner, J., Lu, H., White, I., King, J.C., Phillips, T., Hosking, J.S., Bracegirdle, T.J., Marshall, G.J., Mulvaney, R., Deb, P., 2016. Absence of 21st century warming on Antarctic Peninsula consistent with natural variability Since the 1950s, research stations on the Antarctic Peninsula have recorded some of the largest increases in near-surface air temperature in the Southern Hemisphere. Nature 535, 1–1. doi:10.1038/nature18645

van de Poll, W.H., Lagunas, M., de Vries, T., Visser, R.J.W., Buma, A.G.J., 2011. Non-photochemical quenching of chlorophyll fluorescence and xanthophyll cycle responses after excess PAR and UVR in Chaetoceros brevis, Phaeocystis antarctica and coastal Antarctic phytoplankton. Mar. Ecol. Prog. Ser. 426, 119–131. doi:10.3354/meps09000

van Heukelem, L., Thomas, C.S., 2001. Computer-assisted high-performance liquid chromatography method development with applications to the isolation and analysis of phytoplankton pigments. J. Chromatogr. A 910, 31–49. doi:10.1016/S0378-4347(00)00603-4

van Leeuwe, M.A., Visser, R.J.W., Stefels, J., 2014. The pigment composition of Phaeocystis antarctica (Haptophyceae) under various conditions of light, temperature, salinity, and iron. J. Phycol. 50,

1070–1080. doi:10.1111/jpy.12238

Venables, H.J., Clarke, A., Meredith, M.P., 2013. Wintertime controls on summer stratification and productivity at the western Antarctic Peninsula. Limnol. Oceanogr. 58, 1035–1047. doi:10.4319/lo.2013.58.3.1035

Venables, H.J., Meredith, M.P., 2014. Feedbacks between ice cover, ocean stratification, and heat content in Ryder Bay, western Antarctic Peninsula. J. Geophys. Res. Ocean. 119, 5323–5336. doi:10.1002/jgrc.20224

Wang, Q., Garrity, G.M., Tiedje, J.M., Cole, J.R., 2007. Naive Bayesian classifier for rapid assignment of rRNA sequences into the new bacterial taxonomy. Appl. Environ. Microbiol. 73, 5261–7. doi:10.1128/AEM.00062-07

Williams, T.J., Long, E., Evans, F., Demaere, M.Z., Lauro, F.M., Raftery, M.J., Ducklow, H., Grzymski, J.J., Murray, A.E., Cavicchioli, R., 2012. A metaproteomic assessment of winter and summer bacterioplankton from Antarctic Peninsula coastal surface waters. ISME J. 6, 1883–900. doi:10.1038/ismej.2012.28

Wolf, C., Frickenhaus, S., Kilias, E.S., Peeken, I., Metfies, K., 2013. Protist community composition in the Pacific sector of the Southern Ocean during austral summer 2010. Polar Biol. 1–15. doi:10.1007/s00300-013-1438-x

Wood, L.W., 1985. Chloroform–methanol rxtraction of chlorophyll a. Can. J. Fish. Aquat. Sci. 42, 38–43. doi:10.1139/f85-005

Wright, S.W., Ishikawa, A., Marchant, H.J., Davidson, A.T., van den Enden, R.L., Nash, G. V., 2009. Composition and significance of picophytoplankton in Antarctic waters. Polar Biol. 32, 797–808. doi:10.1007/s00300-009-0582-9

Wright, S.W., van den Enden, R.L., Pearce, I., Davidson, A.T., Scott, F.J., Westwood, K.J., 2010. Phytoplankton community structure and stocks in the Southern Ocean (30-80°E) determined by CHEMTAX analysis of HPLC pigment signatures. Deep. Res. Part II Top. Stud. Oceanogr. 57, 758–

778. doi:10.1016/j.dsr2.2009.06.015

Yu, L., Zhang, W., Liu, L., Yang, J., 2015. Determining Microeukaryotic Plankton Community around Xiamen Island, Southeast China, Using Illumina MiSeq and PCR-DGGE Techniques. PLoS One 10, e0127721. doi:10.1371/journal.pone.0127721

Zhang, J., Kobert, K., Flouri, T., Stamatakis, A., 2014. PEAR: A fast and accurate Illumina Paired-End reAd mergeR. Bioinformatics 30, 614–620. doi:10.1093/bioinformatics/btt593

Zhu, F., Massana, R., Not, F., Marie, D., Vaulot, D., 2005. Mapping of picoeucaryotes in marine ecosystems with quantitative PCR of the 18S rRNA gene. FEMS Microbiol. Ecol. 52, 79–92. doi:10.1016/j.femsec.2004.10.006

Tables

Table 1: Diversity indices retrieved from the DGGE analysis. The parameters were calculated from the number of bands and relative intensity per band per sample. At the bottom, the averages and standard deviations (Stdev) are presented.

	Eukaryotes			Diatoms			Dinoflagellates			Bacteria		
	# Species	Evenness	Simpson	# Species	Evenness	Simpson	# Species	Evenness	Simpson	# Species	Evenness	Simpson
09 Dec	28	0.64	0.93	16	0.56	0.85	20	0.64	0.90	24	0.64	0.92
13 Jan	29	0.77	0.94	15	0.64	0.86	17	0.55	0.84	25	0.69	0.93
24 Jan	26	0.73	0.93	10	0.60	0.77	21	0.70	0.92	21	0.58	0.86
27 Jan	34	0.70	0.95	16	0.63	0.88	17	0.69	0.89	29	0.62	0.92
31 Jan	29	0.79	0.95	8	0.71	0.79	20	0.78	0.92	23	0.80	0.93
03 Feb	21	0.73	0.92	12	0.65	0.83	21	0.74	0.92	21	0.69	0.91
10 Feb	30	0.69	0.93	12	0.68	0.85	24	0.68	0.92	24	0.61	0.90
16 Feb	25	0.68	0.92	16	0.78	0.91	17	0.75	0.90	22	0.67	0.91
21 Feb	27	0.83	0.95	11	0.64	0.82	20	0.74	0.92	20	0.65	0.89
Average	28	0.73	0.94	13	0.65	0.84	20	0.70	0.90	23	0.66	0.91
Stdev	3	0.06	0.01	3	0.06	0.04	2	0.06	0.02	3	0.06	0.02

Table 2: Dominant eukaryote genera which represent nodes observed >1% of the total number of sequences of the three samples combined. All numbers are percentages and the sum per sample is presented at the bottom.

	Sampling Date		
	9 Dec	27 Jan	16 Feb
Thalassiosira	15.83	36.75	46.36
Unassigned Bacillariophyceae	33.74	0.72	4.03
Unassigned Alveolata	4.73	12.97	8.05
Unassigned Mediophyceae	3.53	5.44	14.07
Unassigned Dinophyceae	10.27	5.54	1.95
Unassigned Gymnodiniphycidae	2.36	10.68	4.38
Unassigned Dinoflagellata	2.68	5.30	6.68
Maxillopoda	0.05	8.44	0.50
Unassigned Eukaryotes	1.24	1.77	3.84
Unassigned Animalia	0.47	2.68	1.11
Chaetoceros	0.52	1.21	2.37
Mast-4 Stramenopiles	3.20	0.15	0.39
Unassigned Stramenopiles	3.44	0.06	0.08
Unassigned Bacillariophytina	3.21	0.10	0.23
Unassigned Prymnesiophyceae	0.60	1.21	1.24
Unassigned Choreotrichia	2.01	0.29	0.11
Protaspa	2.05	0.21	0.11
Unassigned Thecofilosea	1.13	0.60	0.48
Unassigned Cryptomonadales	1.59	0.20	0.08
Stellarima microtrias	0.08	1.38	0.31
Unassigned Diatomea	0.90	0.30	0.55
Unassigned Oligotrichia	1.12	0.19	0.26
Unassigned Syndiniales Group I	1.32	0.07	0.13
MAST-1 Stramenopiles	0.45	0.37	0.43
Sum	96.52	96.63	97.74
Total sequences entire sample	63493	53079	35361

Figure Legends

Fig. 1: Map of sampling area: (Left) the position of Rothera research station on Adelaide Island, north of Marguerite Bay and (Right) the RaTS sampling site in Ryder Bay near Rothera research station.

Fig. 2. Plots of the salinity (Top), temperature (Middle), and fluorescence and density (Bottom) during the spring and summer period. Density (Bottom) is marked by the black isobar lines. The horizontal dashed line indicates 15-m depth, whereas the vertical lines indicate sampling days.

Fig. 3: (Top) Wind speed and MLD during the spring and summer. Wind speed (thin black line) is a 5-day running average. MLD (black dashed line). (Bottom) Salinity (black dots) and meteoric water (white dots) content at 15 m.

Fig. 4: Concentrations of macronutrients ((Top) Nitrate + Nitrite (black dots), Phosphate (white dots) and (Bottom) Silicate) as measured at 15 m in μM. The bottom graph has the N/P ratios included. N in this ratio is Nitrate + Nitrite. The solid line marks the classical Redfield ratio (Redfield, 1958).

Fig. 5: Phytoplankton biomass and composition based on HPLC measurements analysed with CHEMTAX. Total Chl-a is indicated by the solid line. The fraction microplankton is indicated by the dashed line. Asterisks mark DNA sampling days. The different periods in the Antarctic summer, as discussed in 4.1, are marked above the graph.

Fig. 6: NMDS biplots (Left) and dendrograms (Right) of eukaryotes (Top) and diatoms (Bottom). Dendrograms and NMDSs' are based on the Bray-Curtis similarity coefficient. Black dots in the NMDS represent the DGGE results for a given sampling event. Grey arrows indicate environmental parameters. Stress according to Shepard plots was 0.20 for eukaryotes and 0.18 for diatoms.

Numbers at the branches of the clusters show the bootstrap percentage (n = 1000). Clusters discussed in this paper are marked and named.

Fig. 7: NMDS biplots (Left) and dendrograms (Right) of dinoflagellates (Top) and Bacteria (Bottom). Dendrograms and NMDSs' are based on the Bray-Curtis similarity coefficient. Black dots in the NMDS represent the DGGE results for a given sampling event. Stress according to Shepard plots was 0.06 for dinoflagellates and 0.10 for bacteria. Grey arrows indicate environmental parameters. Numbers at the branches of the clusters show the bootstrap percentage (n = 1000). Clusters discussed in this paper are marked and named.

Fig. 8: DNA sequences shown per major phytoplankton group. The diatom groups are segregated into their order when possible. More descriptive names (Polar, pennate and radial centric diatoms) are given in the legend as derived from Medlin and Kaczmarska (2004).

Fig. 9: Bacterial community composition derived from 16S rRNA gene amplicon sequencing analysis. Stacked column graph represents the relative distribution of the dominant classes at the different time points. The total number of sequence reads was 63493, 53079 and 35361 per sample for respectively 9 December, January 27 and February 16.

Figure 1

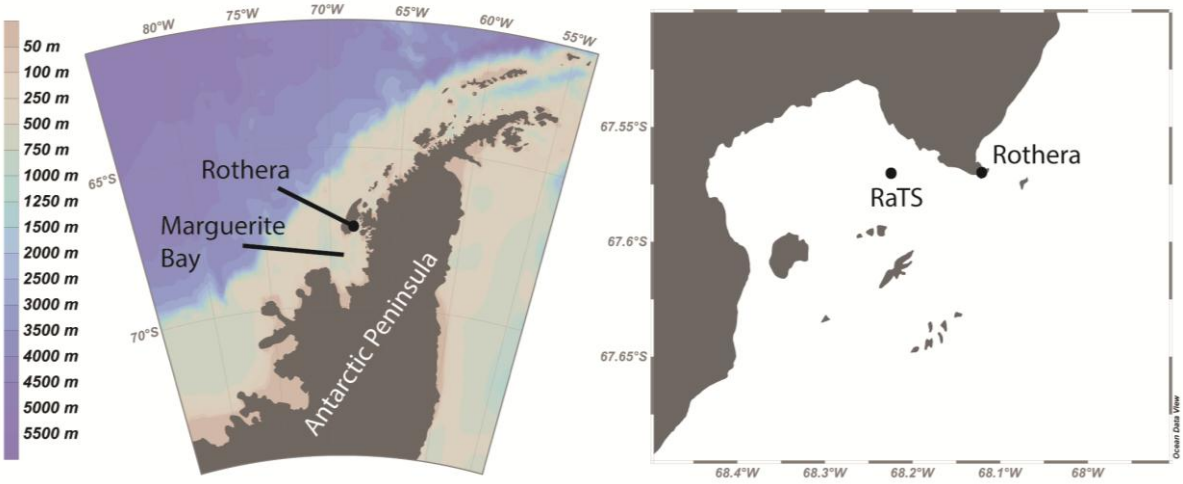

Figure 2

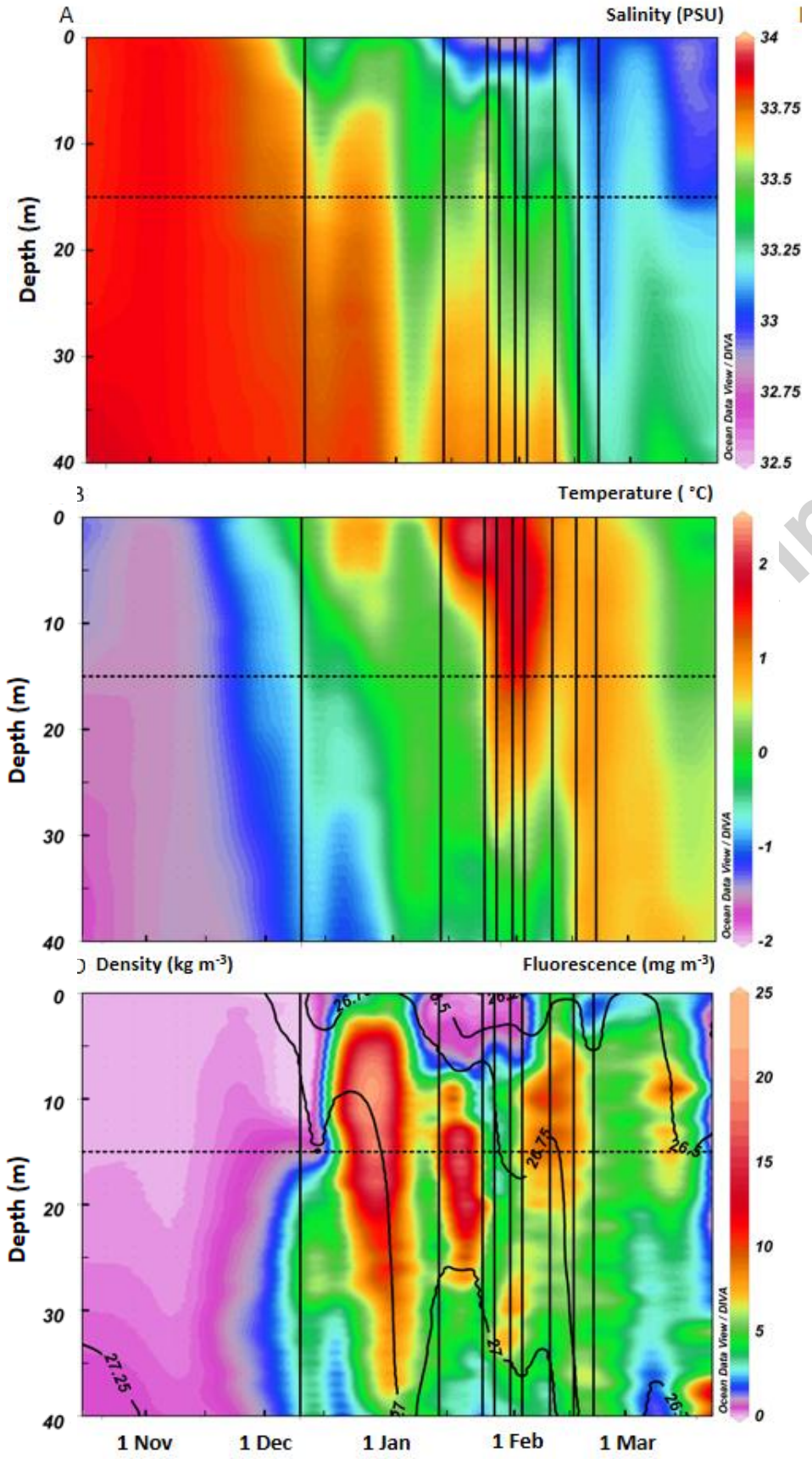
A
Salinity (PSU)
Depth (m)
0
10
20
30
40
34
33.75
33.5
33.25
33
32.75
32.5
Ocean Data View / DIVA
Temperature (°C)
2
1
0
-1
-2
Density (kg m-3)
Fluorescence (mg m-3)
25
20
15
10
5
0
26.75
27.25
1 Nov
1 Dec
1 Jan
1 Feb
1 Mar

Figure 3

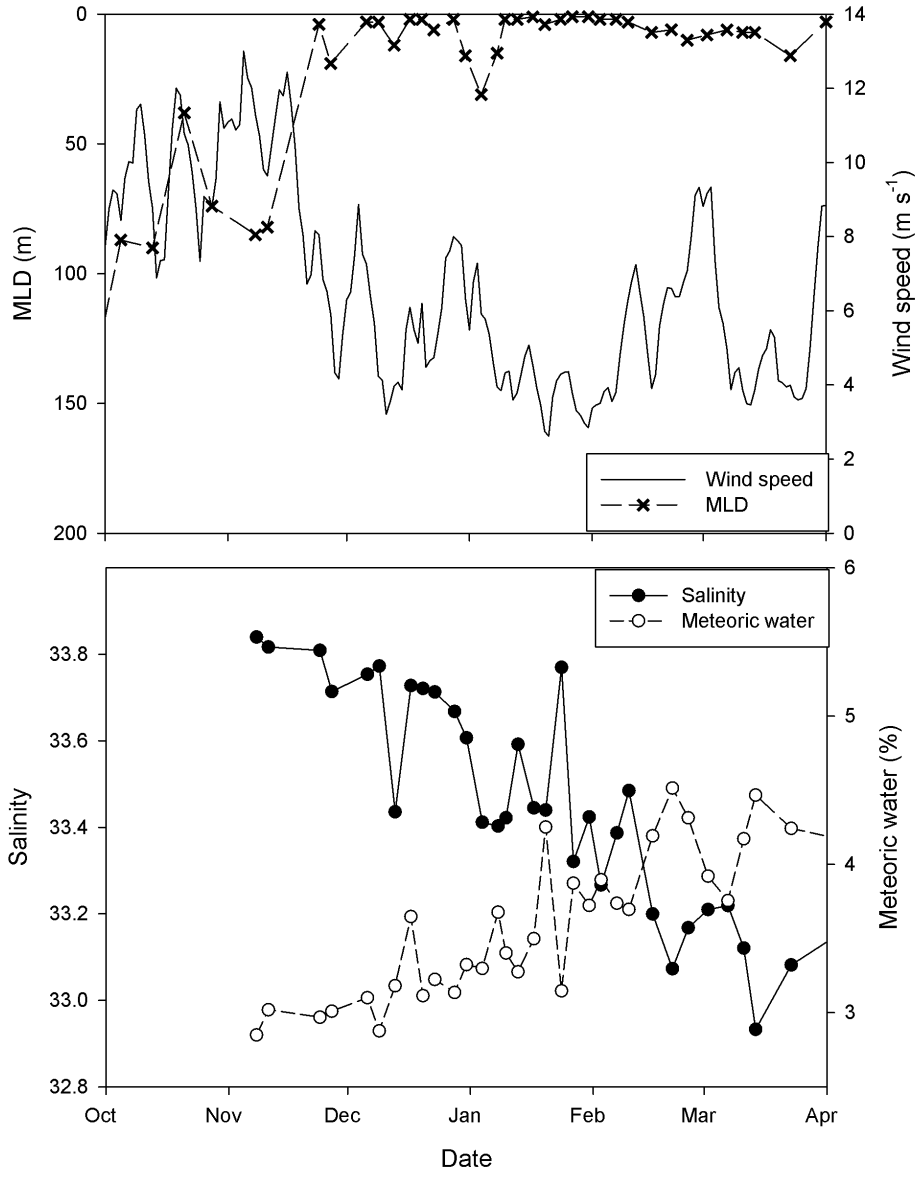
MLD (m)
Wind speed (m s-1)
Wind speed
MLD
Salinity
Meteoric water (%)
Salinity
Meteoric water
Oct
Nov
Dec
Jan
Feb
Mar
Apr
Date

Figure 4

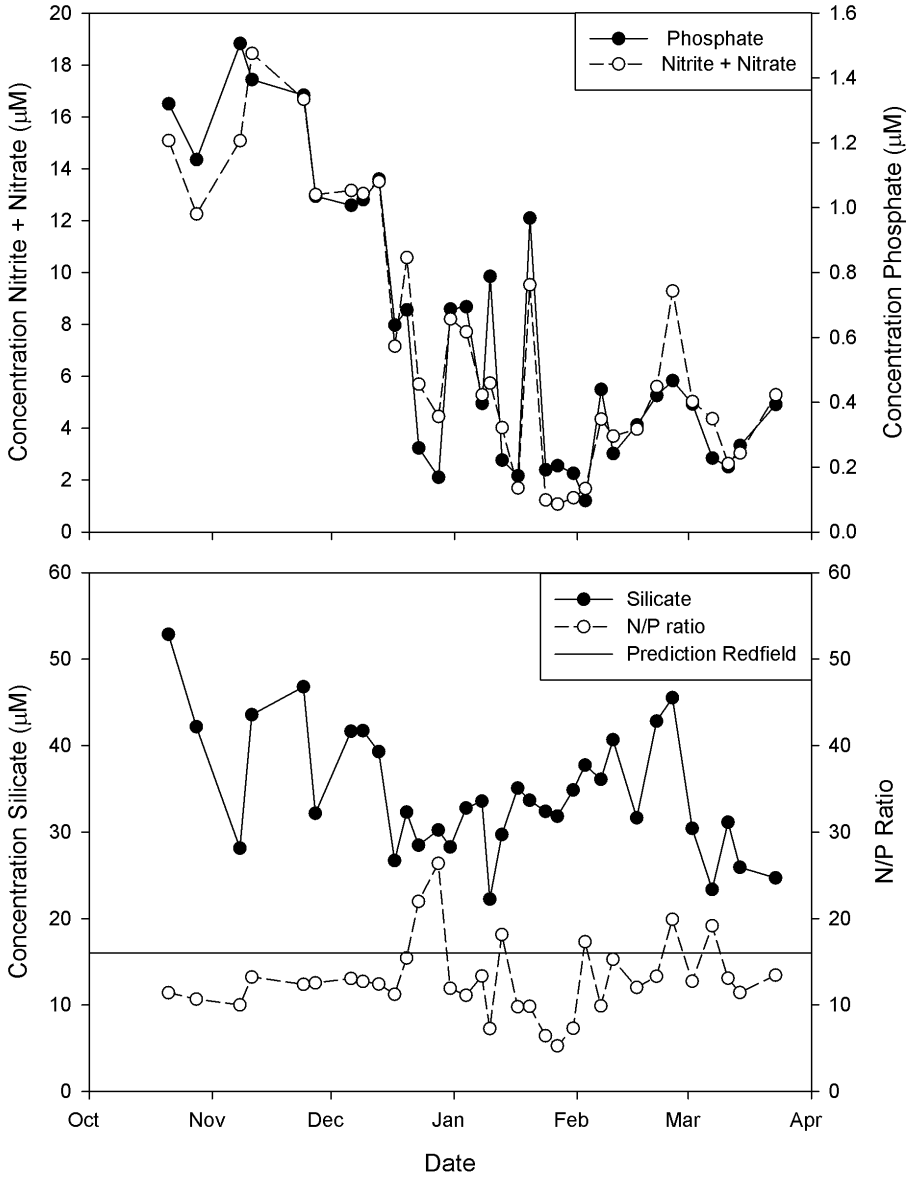

Figure 5

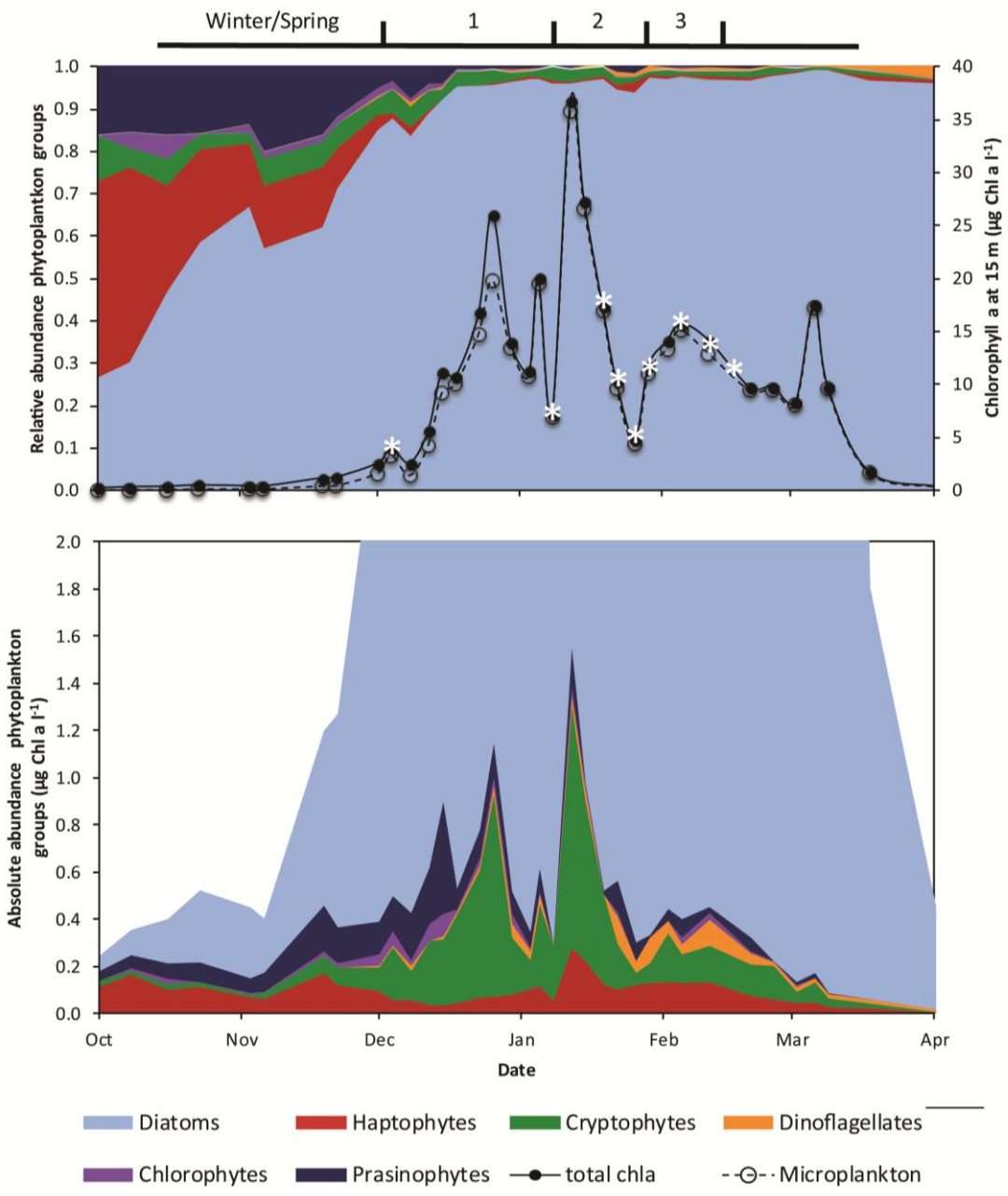
Winter/Spring
1
2
3
Relative abundance phytoplantkon groups
Chlorophyll a at 15 m (µg Chl a l-1)
Absolute abundance phytoplankton groups (µg Chl a l-1)
Oct
Nov
Dec
Jan
Feb
Mar
Apr
Date
Diatoms
Haptophytes
Cryptophytes
Dinoflagellates
Chlorophytes
Prasinophytes
total chla
Microplankton

Figure 6

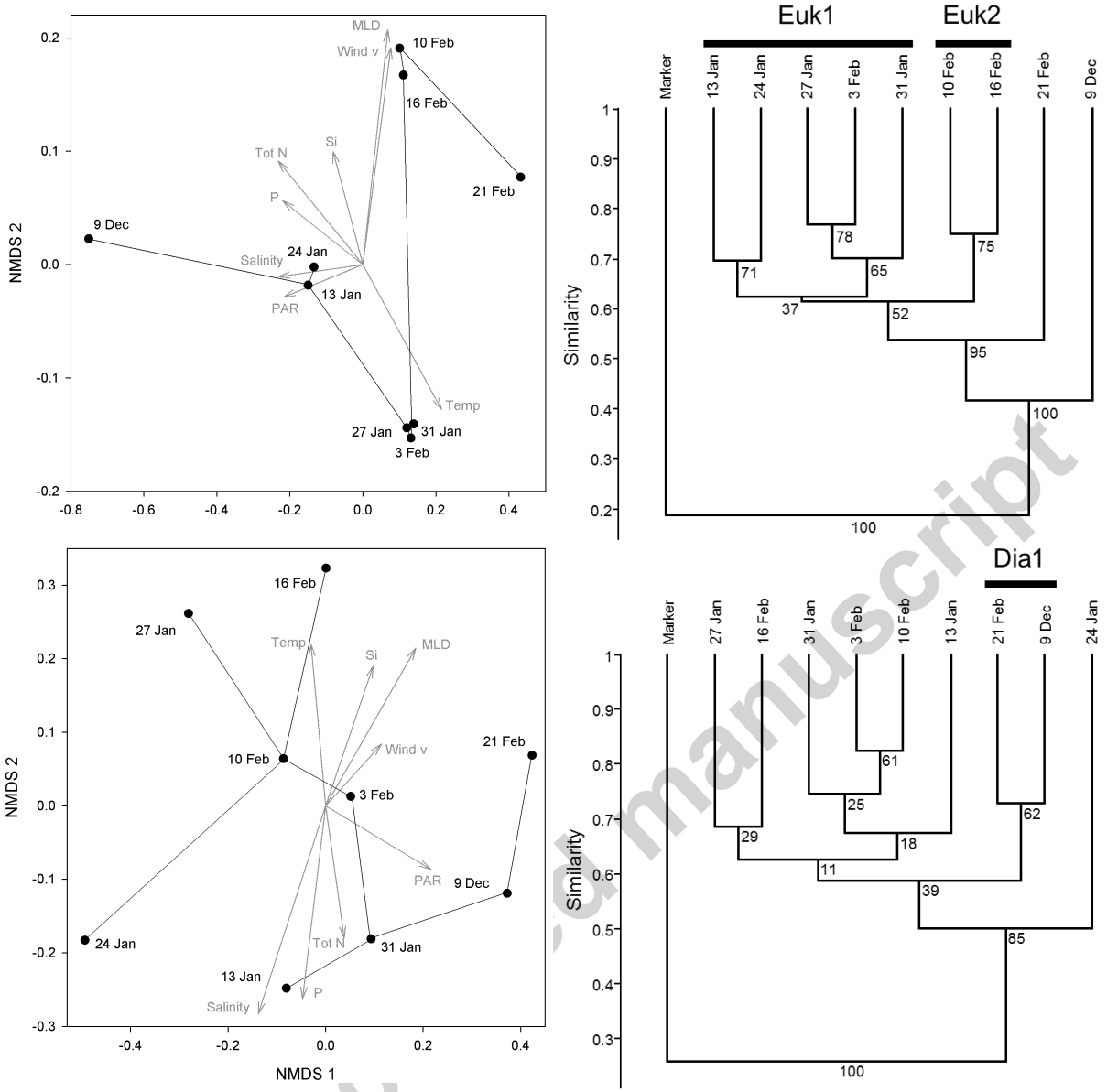

Figure 7

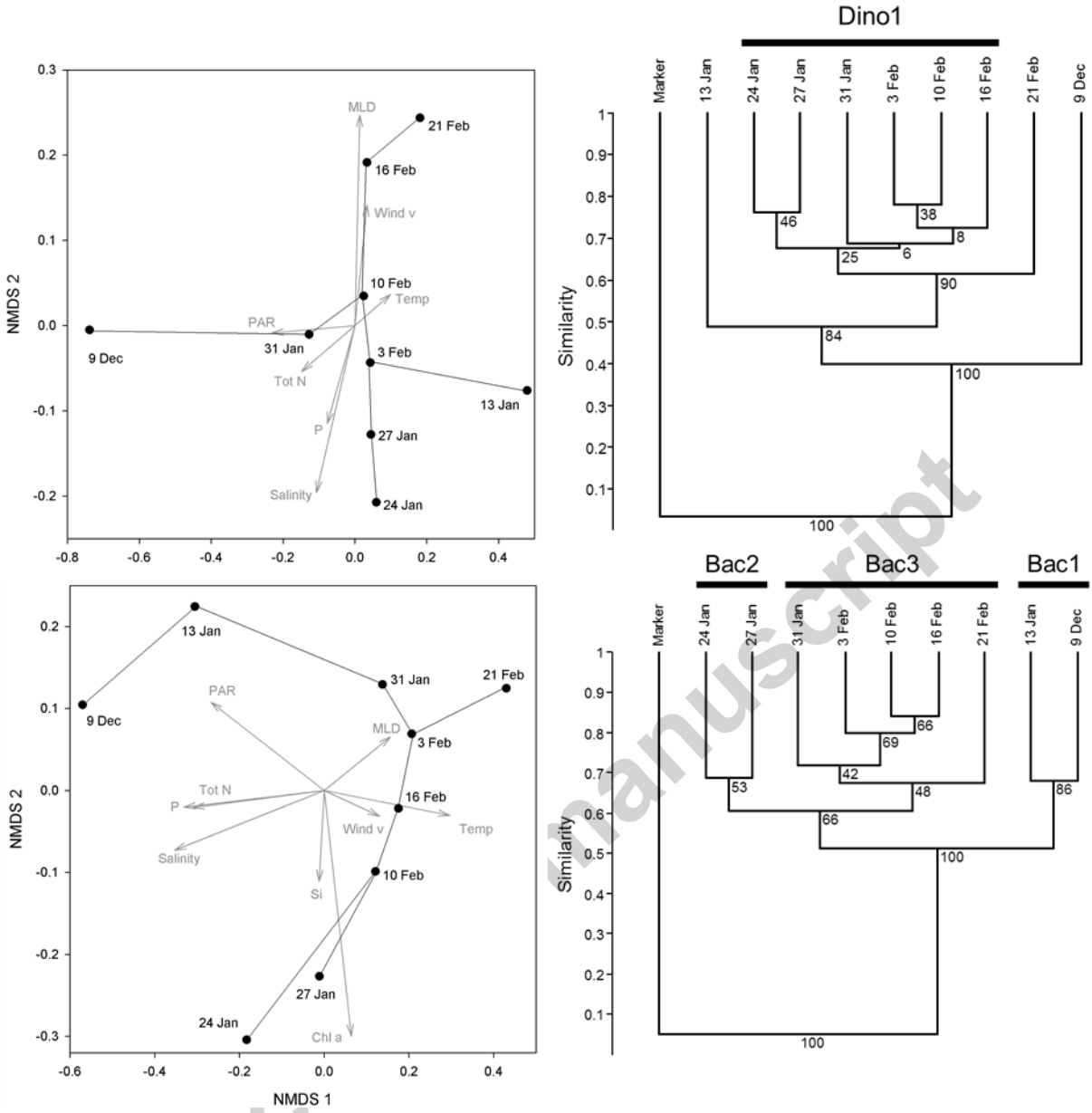

Figure 8

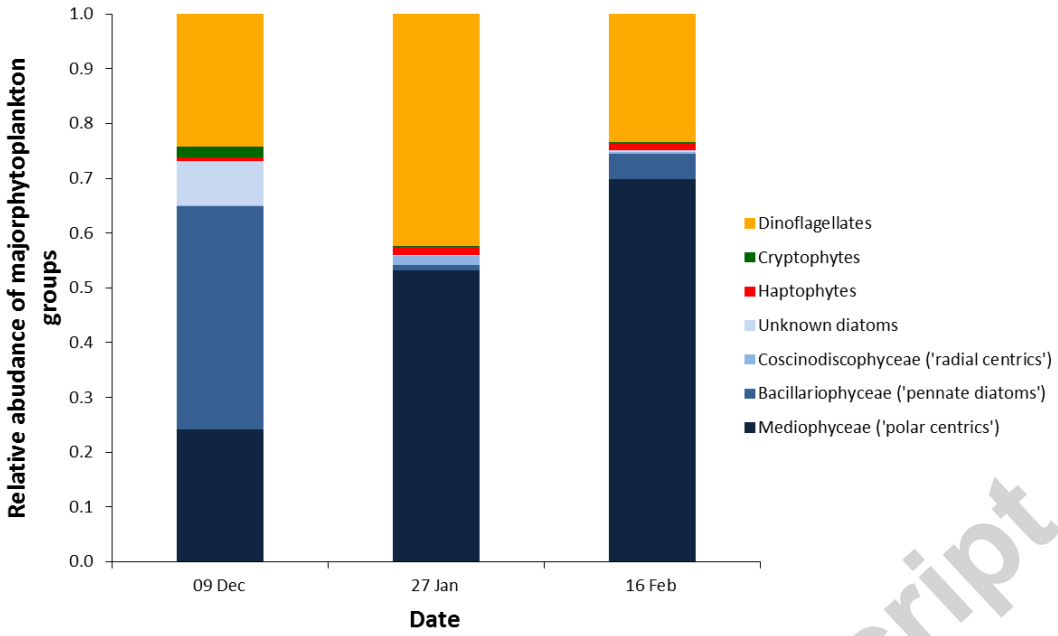

Figure 9

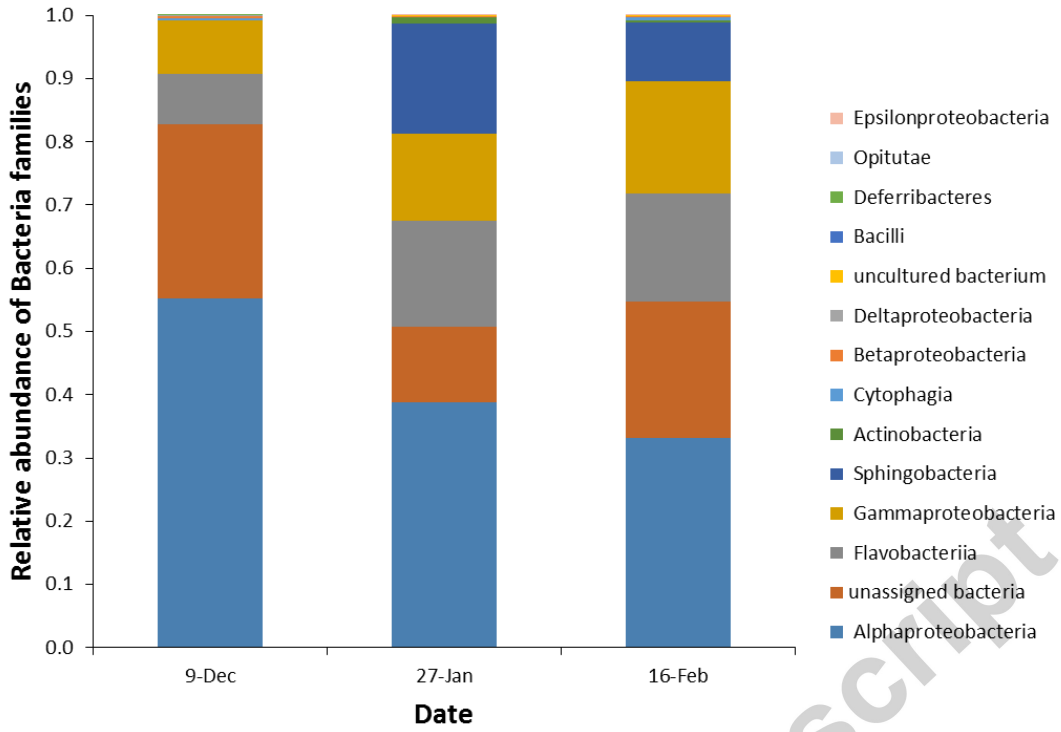

Appendices

Table A.1: Pigment:Chl-a ratios as used in the CHEMTAX analysis. Initial ratios were modified from Wright et al. (2009, 2010). Final ratios were optimized after analysis. Abbreviations: Chl, chlorophyll; Peri, peridinin; Fuco, fucoxanthin; neo, neoxanthin; pras, prasinoxanthin; 19'-hex, 19'-hexanoylfucoxanthin; allo, alloxanthin; 19'-buta, 19'-butanoyloxyfucoxanthin.

Initial ratio Class / Pigment	Chl c3	peri	19'-buta	fuco	neo	pras	19'-hex	allox	Lutein	Chl b	Chl-a
Prasinophytes	-	-	-	-	0.03	0.10	-	-	0.01	0.62	1.00
Chlorophytes	-	-	-	-	0.06	-	-	-	0.22	0.18	1.00
Dinoflagellates	-	1.06	-	-	-	-	-	-	-	-	1.00
Cryptophytes	-	-	-	-	-	-	-	0.22	-	-	1.00
Haptophytes 1	0.13	-	0.12	0.08	-	-	0.40	-	-	-	1.00
Haptophytes 2	0.27	-	0.01	0.01	-	-	1.10	-	-	-	1.00
Diatoms A	-	-	-	0.52	-	-	-	-	-	-	1.00
Diatoms B	0.03	-	-	0.61	-	-	-	-	-	-	1.00
Final Ratio											
Prasinophytes	-	-	-	-	0.03	0.11	-	-	0.01	0.47	1.00
Chlorophytes	-	-	-	-	0.06	-	-	-	0.22	0.18	1.00
Dinoflagellates	-	1.06	-	-	-	-	-	-	-	-	1.00
Cryptophytes	-	-	-	-	-	-	-	0.22	-	-	1.00
Haptophytes 1	0.21	-	0.29	0.13	-	-	0.40	-	-	-	1.00
Haptophytes 2	0.27	-	0.01	0.01	-	-	1.10	-	-	-	1.00

Diatoms A	-	-	-	0.51	-	-	-	-	-	-	1.00
Diatoms B	0.06	-	-	0.64	-	-	-	-	-	-	1.00

Table A.2: The 16S and 18S primers used for DGGE and MiSeq analysis. GC indicates to which primer a GC clamp was attached for DGGE.

	Specificity	Primer name	# Nucleotides	Primer sequence, 5' - 3'	Reference
DGGE	Eukaryotes	Euk 1A	550	CTGGTTGATCCTGCCAG	(Sogin and Gunderson, 1987)
		516 R GC		ACCAGACTTGCCCTCC	(Amann et al., 1990)
	Diatoms	1209 F GC	250	CAGGTCTGTGATGCCCTT	(Giovannoni et al., 1988)
		Diatom18SR1		CAATGCAGWTTGATGAWCTG	(Godhe et al., 2008)
	Dinoflagellates	Dino 18S GC F1	650	AAGGGTTGTGTTYATTAGNTACARAAC	(Lin et al., 2006)
		Dino 18S R1		GAGCCAGATRCDCACCCA	(Lin et al., 2006)
	Bacteria	968 F GC	550	CCTACGGGAGGCAGCAG	(Nübel et al., 1996)
		1401 R		CGGTGTGTACAAGACCC	(Nübel et al., 1996)
MiSeq	Bacteria	28 F	-	GAGTTTGATCNTGGCTCAG	(Frank et al., 2013)
		519 R		GTNTTACNGCGGCKGCTG	(Frank et al., 2013)
	Eukaryotes	Euk A7 F	-	AACCTGGTTGATCCTGCCAGT	(Medlin et al., 1988)
		Euk555 R		GCTGCTGGCACCAGACT	(Moreno et al., 2010)

Table A.3: PCR conditions and composition per primer set. Concentrations are noted as final concentrations

PCR reaction components	Eukaryotes	Diatoms	Dinoflagellates	Bacteria
PCR buffer (Eurogentec)	1x	1x	1x	1x
$MgCl_2$ (Eurogentec)	3.25 mM	2.00 mM	3.25 mM	3.25 mM
Formamide	1%	1%	1%	1%
dNTP's (Eurogentec)	0.2 mM	0.2 mM	0.2 mM	0.2 mM
Primer F (Eurogentec)	0.3 mM	0.3 mM	0.3 mM	0.2 mM
Primer R (Eurogentec)	0.3 mM	0.3 mM	0.3 mM	0.2 mM
Taq Polymerase (Diamond taq, Eurogentec)	2.5 U	2.5 U	2.5	1 U
PCR conditions				
Initial denaturation	130 sec at 94°C	300 sec at 94°C	180 sec at 94°C	300 sec at 94°C
# cycles touchdown PCR			10	10
Denaturation			45 sec at 94°C	60 sec at 94°C
Annealing			60 sec at 63°C-58°C	60 sec at 65°C-55°C
Elongation			180 sec at 72°C	120 sec at 72°C
# cycles main PCR	30	30	30	20
Denaturation	30 sec at 94°C	60 sec at 94°C	45 sec at 94°C	60 sec at 94°C
Annealing	45 sec at 56°C	60 sec at 57°C	60 sec at 58°C	60 sec at 55°C
Elongation	130 sec at 72°C	60 sec at 72°C	180 sec at 72°C	120 sec at 72°C
Final elongation	440 sec at 72°C	300 sec at 72°C	7 min at 72°C	30 min at 72°C

Table A.4: A list of all the observed eukaryotes in our sequencing results. Values represent percentage of the total number of sequences per sample.

	09-12-2010	27-01-2011	16-02-2011
Thalassiosira	15.83	36.75	46.36
Unassigned Bacillariophyceae	33.74	0.72	4.03
Unassigned Alveolata	4.73	12.97	8.05
Unassigned Mediophyceae	3.53	5.44	14.07
Unassigned Dinophyceae	10.27	5.54	1.95
Unassigned Gymnodiniphycidae	2.36	10.68	4.38
Unassigned Dinoflagellata	2.68	5.30	6.68
Maxillopoda	0.05	8.44	0.50
Unassigned Eukaryotes	1.24	1.77	3.84
Unassigned Animalia	0.47	2.68	1.11
Chaetoceros	0.52	1.21	2.37
Mast-4 Stramenopiles	3.20	0.15	0.39
Unassigned Stramenopiles	3.44	0.06	0.08
Unassigned Bacillariophytina	3.21	0.10	0.23
Unassigned Prymnesiophyceae	0.60	1.21	1.24
Unassigned Choreotrichia	2.01	0.29	0.11
Protaspa	2.05	0.21	0.11
Unassigned Thecofilosea	1.13	0.60	0.48
Unassigned Cryptomonadales	1.59	0.20	0.08
Stellarima microtrias	0.08	1.38	0.31
Unassigned Diatomea	0.90	0.30	0.55
Unassigned Oligotrichia	1.12	0.19	0.26
Unassigned Syndiniales Group I	1.32	0.07	0.13
MAST-1 Stramenopiles	0.45	0.37	0.43
Unassigned Peridiniales	0.53	0.22	0.16
Unassigned Pyramimonas	0.67	0.07	0.11
Unassigned Picomonadea	0.04	0.30	0.25
MAST-1A Stramenopiles	0.03	0.18	0.28
MAST-3 Stramenopiles	0.12	0.22	0.13
Pectinoida	0.00	0.46	0.00
Unassigned Micromonas	0.45	0.00	0.00
Unassigned Bolidomonas	0.43	0.01	0.01
Cryptocaryon	0.00	0.37	0.08
Unassigned Palpitomonas	0.22	0.15	0.07
Unassigned Telonema	0.19	0.15	0.09
Unassigned SAR	0.04	0.13	0.16
Pelagostrobilidium	0.26	0.04	0.00
MAST-3L Stramenopiles	0.02	0.02	0.23
Unassigned Haplozoon	0.00	0.21	0.03
Cyrtophoria	0.00	0.19	0.03
Unassigned Picomonadida	0.03	0.09	0.09
Pseudotontonia	0.03	0.11	0.04

Unassigned Labyrinthulomycetes	0.05	0.03	0.09
Unassigned Prymnesiales	0.04	0.01	0.12
Euplotes	0.00	0.09	0.06
Unassigned Chrysophyceae	0.00	0.05	0.09
Unassigned Echinodermata	0.00	0.13	0.01
Corethron	0.09	0.00	0.00
Unassigned Haptoria	0.00	0.07	0.01
Unassigned Ochrophyta	0.07	0.00	0.01
Unassigned Chloroplastida	0.07	0.00	0.00
Unassigned Acanthoecida	0.05	0.01	0.01
Unassigned Centrohelida	0.00	0.00	0.06
Unassigned Ctenophora	0.00	0.04	0.01
Unassigned Thraustochytriaceae	0.00	0.00	0.04
MAST-2 Stramenopiles	0.04	0.00	0.00